

Imido-P(V) Trianion Supported Enantiopure Neutral Tetrahedral Pd(II) Cages

Prabhakaran Rajasekar,^a Swechchha Pandey,^c Harshad Paithankar,^a Jeetender Chugh*,^a
Alexander Steiner^d and Ramamoorthy Boomishankar*,^{a,b}

^aDepartment of Chemistry and ^bCentre for Energy Science, Indian Institute of Science Education and Research (IISER), Pune, Dr. Homi Bhabha Road, Pune – 411008, India

^cPolymer Science and Engineering Division, CSIR-National Chemical Laboratory, Dr. Homi Bhabha Road, Pune – 411008, India

^dDepartment of Chemistry, University of Liverpool, Crown Street, Liverpool – L69 7ZD, U.K.

Table of Contents

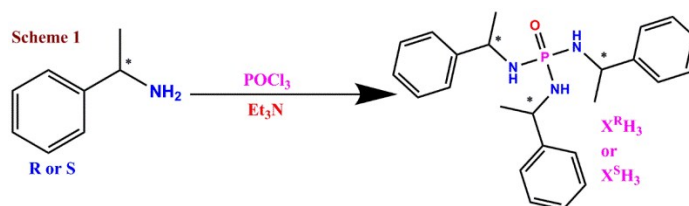
SI. No.	Section	Page Nos.
1	Experimental Section	2-3
2	Crystallography	4-7
3	Characterization data for the ligands	8-10
4	Spectral data for the chiral tetrahedral cages	10-12
5	Structural illustrations and analysis of 1-R and 1-S	12-14
6	Spectral data for the guest-encapsulated chiral tetrahedral cages	15-21
7	Structural illustrations of $\pm\text{bbl}\subset\pm\mathbf{1}$	22-23
8	Low Pressure Gas Sorption Studies	23-24
9	GC Methods for the Enantiomeric Separation of the Chiral Guest Molecules	25-33
10	Optical, spectral and structural data for guest-desorbed cages	32-33
11	Supplementary References	33

Experimental Section

General Remarks

All manipulations involving phosphorus halides were performed under dry nitrogen atmosphere in standard Schlenk glassware. Dry Solvents were purchased from local vendors and used without further purification. The Chiral amines, oxalic acid, palladium acetate were purchased from Aldrich and used as received. POCl_3 was purchased locally and was distilled prior to use. The ligand $\text{X}^{\text{R}}\text{H}_3$ was synthesized according to the earlier reported procedure.¹ NMR spectra were recorded on a Jeol 400 MHz spectrometer (^1H NMR: 400.13 MHz, ^{13}C {1 H} NMR: 100.62 MHz, ^{31}P {1 H} NMR: 161.97 MHz) or on a Bruker 400 MHz (1 H NMR: 500.00 MHz, ^{13}C {1 H} NMR: 125.725 MHz, ^{31}P {1 H} NMR: 202.404 MHz) spectrometer at room temperature using TMS (^1H , ^{13}C) and 85% H_3PO_4 (^{31}P). The mass spectra were obtained on an Applied Bio system matrix-assisted laser desorption ionization time-of-flight (MALDI-TOF)/TOF spectrometer. Thermal analysis (TGA) data have been obtained from a PerkinElmer STA-6000 thermo gravimetric analyzer. CD spectra were measured in JASCO J815 spectrometer from 400 nm – 190 nm. Elemental analyses were performed on a Vario-EL cube elemental analyzer. GC was performed on Agilent 7890B GC system using Supelco β -dex 225 (30 m* 0.25 mm * 0.25 μm) and Supelco γ -dex (30 m* 0.25 mm * 0.25 μm) columns, Split ratio 30:1, FID temperature 300 $^\circ\text{C}$.

1. General synthesis of chiral phosphoramides



Scheme S1: Synthesis of the chiral phosphoramidate ligands.

To a stirred solution of R or S alpha-methyl benzyl amine (1.25 ml, 9.72mmol) and triethylamine (1.35ml, 9.72mmol) in dichloromethane (15ml) at 0°C was added POCl_3 (0.3ml, 3.24mmol) drop wise. The resultant mixture was slowly brought to room temperature and stirred for an over-night period. The precipitated triethylamine hydrochloride salt was filtered and the solution was evaporated to obtain the crude phosphoramidate as an oily substance. This was further purified on a silica gel column using dichloromethane and methanol as an elutant to obtain a colorless solid.

$\text{X}^{\text{R}}\text{H}_3$: Yield: 84% (1.15 gm, based on P). ^1H NMR (400 MHz, CDCl_3): δ 1.35 (d, 9H, CH_3), 4.3-4.40(m, 3H, CH), δ 2.45 (t, 3H, NH), 7.15-7.30 (m, 15H, aromatic). ^{13}C NMR (100 MHz, CDCl_3): δ 25.6, 51.0, 125.7, 126.9, 128.5, 145.7. ^{31}P NMR (161 MHz, CDCl_3): δ 11.07. MALDI-TOF/TOF: 446 (M+K)⁺.

$\text{X}^{\text{S}}\text{H}_3$: Yield: 80% (1.05 gm, based on P). ^1H NMR (400 MHz, CDCl_3): δ 1.35 (d, 9H, CH_3), 4.3-4.40(m, 3H, CH), δ 2.45 (t, 3H, NH), 7.15-7.30 (m, 15H, aromatic). ^{13}C NMR (100 MHz, CDCl_3): δ 25.6, 51.0, 125.7, 126.9, 128.5, 145.7. ^{31}P NMR (161 MHz, CDCl_3): δ 11.07. MALDI-TOF/TOF: 446 (M+K)⁺.

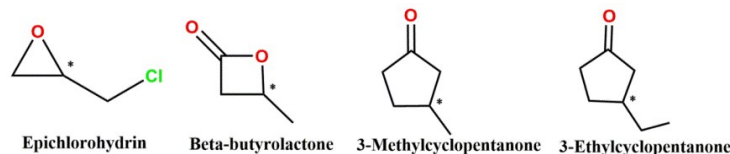
2.Preparation of Enantiopure chiral Tetrahedral Cages (1-R) or (1-S): The Ligand $X^R\text{H}_3$ or $X^S\text{H}_3$ (20 mg, 0.049 mmol) and Palladium acetate (33 mg, 0.147 mmol) and oxalic acid (9 mg, 0.073 mmol) in DMSO (2ml) were heated to 60°C for 1 hr to yielded an orange colored precipitate. The precipitated compound was recovered by filtration, washed with methanol 2-3 times and dried under vacuum. The cage assemblies 2-R or 2-S were crystallised from slow evaporation of its dichloromethane solution in 2 days.

1-R: Yield: 83% (based on P). MALDI-TOF/TOF: 3462 (M+K)⁺. ³¹P NMR (161 MHz, CD₂Cl₂): δ 71.30. ¹H NMR (400 MHz, CD₂Cl₂): δ 1.55 (d, 3H, CH₃), 3.70-3.86 (m, 3H, CH), 7.73-7.80(d, 2H, aromatic), 7.44-7.54(m, 3H, aromatic). ¹³C NMR (100 MHz, CD₂Cl₂): δ 25.7, 63.3, 130.5, 130.5, 131.1, 142.9, 175.6. Elemental Analysis (%): Calcd for C₁₀₈ H₁₀₈ N₁₂ O₂₈ P₄ Pd₁₂: C, 37.90; H, 3.18; N, 4.91. Found: C, 37.80; H, 3.05; N, 4.82;

1-S: Yield: 81% (based on P). MALDI-TOF/TOF: 3462 (M+K)⁺. ³¹P NMR (161 MHz, CDCl₃): δ 71.30. ¹H NMR (400 MHz, CD₂Cl₂): δ 1.55 (d, 3H, CH₃), 3.70-3.86 (m, 3H, CH), 7.73-7.80(d, 2H, aromatic), 7.44-7.54(m, 3H, aromatic). ¹³C NMR (100 MHz, CD₂Cl₂): δ 25.7, 63.3, 130.5, 130.5, 131.1, 142.9, 175.6. Elemental Analysis (%): Calcd for C₁₀₈ H₁₀₈ N₁₂ O₂₈ P₄ Pd₁₂: C, 37.90; H, 3.18; N, 4.91. Found: C, 37.80; H, 3.05; N, 4.83;

General procedure for encapsulation-separation experiment and resolved results for racemic substrates by 1-R and 1-S.

In a typical encapsulation-separation experiment, excess of racemic guests were separately added to 1-R and 1-S in dry DCM (10ml). For rac-epichlorohydrin (epi) and β-butyrolactone (BBL) the reaction mixture was stirred for 1-h and left for slow evaporation for upto one week. For 3-Methyl cyclopentanone (3-Me-Cp) and 3-Ethyl cyclopentanone (3-Et-Cp), the solutions were heated to 50° C for 2-3 days in tightly screw-capped pressure vials and the resulting DCM solutions were left stranded for evaporation to yield the crystalline solids of the host-guest complexes. The excess of guest molecules were removed from the surface of the complexes by repeated washing with diethyl ether (3-5 times). The adsorbed guest molecules were subsequently removed from the complexes by soaking in MeOH and analyzed by gas chromatography. The GC methods employed in the study along with the GC chromatogram and analysis plots are given in the last section of supporting information document (Figures S27-S38).



Elemental Analysis data of ±epi⊂1-R:

Anal (%). Calcd for C₁₁₁H₁₁₃N₁₂P₄O₂₉Pd₁₂Cl: C, 37.52; H, 3.24; N, 4.78. Found: C, 37.24; H, 3.37; N, 4.85.

Elemental Analysis data of ±bbl⊂1-R:

Anal (%). Calcd for C₁₁₂H₁₁₄N₁₂P₄O₃₀Pd₁₂: C, 38.34; H, 3.30; N, 4.79. Found: C, 38.34; H, 3.24; N, 4.73.

Elemental Analysis data of ±3-Me-cp⊂1-R:

Anal (%). Calcd for C₁₁₄H₁₁₈N₁₂P₄O₂₉Pd₁₂: C, 38.89; H, 3.38; N, 4.77. Found: C, 38.76; H, 3.40; N, 4.83.

Elemental Analysis data of ± 3 -Et-cp \subset **1-R**:

Anal (%). Calcd for $C_{115}H_{120}N_{12}P_4O_{29}Pd_{12}$: C, 39.0; H, 3.50; N, 4.75. Found: C, 38.95; H, 3.43; N, 4.87.

Crystallography

Reflections were collected on a Bruker Smart Apex Duo diffractometer at 100 K using Mo $K\alpha$ radiation ($\lambda = 0.71073 \text{ \AA}$) for ligand $X^S H_3$, **1-R**, **1-S**, $\pm bbl \subset \pm 1$. All structures were solved using intrinsic phasing method, and refined by full-matrix least-squares on F^2 (G. M. Sheldrick, SHELXL, program for crystal structure refinement, University of Göttingen, Germany, 2015).² Crystallographic data for all these compounds are listed in Table S1. All non-hydrogen atoms were refined anisotropically if not stated otherwise. Hydrogen atoms were constrained in geometric positions to their parent atoms. The diffuse solvent molecules in **1-R** and **1-S** could not be modeled appropriately. Hence, these were treated as diffuse contributions to the overall scattering and removed by the SQUEEZE/PLATON for a better refinement data. All the phenyl rings are constrained to ideal six membered rings. The disordered $\pm bbl$ guests in $\pm bbl \subset \pm 1$ were treated with same/sad constraints and refined isotropically.

Table S1: Crystallographic Data for Ligand $X^S H_3$, Cages **1-R** and **1-S**.

Compound	$X^S H_3$	1-R	1-S	$\pm bbl \subset \pm 1$
Chemical formula	$C_{24}H_{30}N_3OP$	$C_{108}H_{108}N_{12}O_{28}P_4Pd_{12}$	$C_{108}H_{108}N_{12}O_{28}P_4Pd_{12}$	$C_{292}H_{330}N_{24}O_{95}P_8Pd_{24}$
Formula weight	407.48	3422.74	3422.74	8497.14
Temperature	100(2)K	100(2)K	100(2)K	100(2)K
Crystal system	trigonal	Cubic	Cubic	Monoclinic
Space group	P 32	F 23	F 23	Cc
a (Å); α (°)	12.209(3); 90	28.28800; 90	28.04600; 90	20.679(2); 90
b (Å); β (°)	12.209(3); 90	28.28800; 90	28.04600; 90	25.531(2); 94.48
c (Å); γ (°)	12.997(3); 120	28.28800; 90	28.04600; 90	31.458(3); 90
V (Å ³); Z	1677.8(9)	22636(67)	22060	16557(3)
ρ (calc.) mg m ⁻³	1.210	1.004	1.031	1.704
μ (Mo $K\alpha$) mm ⁻¹	0.142	0.997	1.023	1.39
$2\theta_{max}$ (°)	56.912	50.006	56.668	56.86
Flack parameter	0.00(14)	0.01(4)	-0.023(18)	0.03(5)
R(int)	0.159	0.152	0.066	0.053
Data / param.	4834/229	4782/113	4648/113	40598/1831
GOF	0.826	1.015	1.05	1.133
R1 [$F > 4\sigma(F)$]	0.066	0.072	0.042	0.068
wR2 (all data)	0.1966	0.0917(3343)	0.1316(4648)	0.1837
Max. peak/hole(e.Å ⁻³)	0.23/ -0.32	2.66/-0.73	0.40/-0.76	1.77/ -1.74

Table S2. Selected bond lengths (Å) and bond angles (°) for **1-R** and **1-S**.

CAGE	Bond Lengths	Bond Angles
1-R	Pd1 N1 2.001(6)	N1 Pd1 N1 76.7(4)
	Pd1 N1 2.004(6)	N1 Pd1 O12 101.2(2)
	Pd1 O12 2.049(5)	N1 Pd1 O12 177.1(2)
	Pd1 O11 2.052(5)	N1 Pd1 O11 175.6(2)
	Pd1 Pd1 3.0966(11)	N1 Pd1 O11 99.5(2)
	Pd1 Pd1 3.0966(19)	O12 Pd1 O11 82.6(2)
	P1 O1 1.431(9)	N1 Pd1 Pd1 39.40(16)
	P1 N1 1.694(7)	N1 Pd1 Pd1 81.19(18)
	P1 N1 1.694(6)	O12 Pd1 Pd1 95.90(15)
	P1 N1 1.694(6)	O11 Pd1 Pd1 138.42(15)
	P1 Pd1 2.721(3)	N1 Pd1 Pd1 81.22(18)
	P1 Pd1 2.721(3)	N1 Pd1 Pd1 39.33(16)
	O11 C11 1.247(8)	O12 Pd1 Pd1 138.75(15)
	O11 Pd1 2.052(5)	O11 Pd1 Pd1 94.44(15)
	O12 C11 1.252(8)	Pd1 Pd1 Pd1 59.999(16)
	N1 C1 1.517(10)	O1 P1 N1 122.2(2)
	N1 Pd1 2.001(6)	O1 P1 N1 122.2(2)
	C11 C11 1.572(15)	N1 P1 N1 94.3(3)
	C3 C4 1.3900	O1 P1 N1 122.2(2)
	C3 C8 1.3900	N1 P1 N1 94.3(3)
	C3 C1 1.521(10)	N1 P1 N1 94.3(3)
	C4 C5 1.3900	O1 P1 Pd1 138.93(6)
	C4 H4 0.9500	N1 P1 Pd1 98.9(2)
	C5 C6 1.3900	N1 P1 Pd1 47.2(2)
	C5 H5 0.9500	N1 P1 Pd1 47.2(2)
	C6 C7 1.3900	O1 P1 Pd1 138.93(5)
	C6 H6 0.9500	N1 P1 Pd1 47.2(2)
	C7 C8 1.3900	N1 P1 Pd1 47.2(2)
	C7 H7 0.9500	N1 P1 Pd1 98.9(2)
	C8 H8 0.9500	Pd1 P1 Pd1 69.36(8)
	C1 C2 1.542(11)	C11 O11 Pd1 111.3(5)
	C1 H1 1.0000	C11 O12 Pd1 111.9(5)
	C2 H2A 0.9800	C1 N1 P1 124.4(5)
	C2 H2B 0.9800	C1 N1 Pd1 119.3(5)
	C2 H2C 0.9800	P1 N1 Pd1 94.5(3)
		C1 N1 Pd1 117.5(5)
		P1 N1 Pd1 94.4(3)
		Pd1 N1 Pd1 101.3(2)
		O11 C11 O12 126.0(7)
		O11 C11 C11 117.6(8)
		O12 C11 C11 116.4(8)
		C4 C3 C8 120.0
		C4 C3 C1 120.9(5)
		C8 C3 C1 119.1(5)
		C3 C4 C5 120.0
		C3 C4 H4 120.0
		C5 C4 H4 120.0
		C6 C5 C4 120.0
		C6 C5 H5 120.0

		C4 C5 H5 120.0 C5 C6 C7 120.0 C5 C6 H6 120.0 C7 C6 H6 120.0 C8 C7 C6 120.0 C8 C7 H7 120.0 C6 C7 H7 120.0 C7 C8 C3 120.0 C7 C8 H8 120.0 C3 C8 H8 120.0 N1 C1 C3 111.8(6) N1 C1 C2 109.6(7) C3 C1 C2 114.6(7) N1 C1 H1 106.8 C3 C1 H1 106.8 C2 C1 H1 106.8 C1 C2 H2A 109.5 C1 C2 H2B 109.5 H2A C2 H2B 109.5 C1 C2 H2C 109.5 H2A C2 H2C 109.5 H2B C2 H2C 109.5
1-S	Pd1 N1 2.016(6) Pd1 N1 2.021(6) Pd1 O1O 2.056(5) Pd1 O2O 2.056(5) Pd1 Pd1 3.090(3) Pd1 Pd1 3.090(3) P1 O1 1.431(9) P1 N1 1.733(7) P1 N1 1.733(7) P1 N1 1.733(7) P1 Pd1 2.746(4) P1 Pd1 2.746(4) O2O C1O 1.242(9) O2O Pd1 2.056(5) O1O C1O 1.248(9) N1 C11 1.492(11) N1 Pd1 2.016(7) C1O C1O 1.581(16) C12 C11 1.547(12) C12 H12A 0.9800 C12 H12B 0.9800 C12 H12C 0.9800 C11 C13 1.529(10) C11 H11 1.0000 C13 C14 1.3900 C13 C18 1.3900 C14 C15 1.3900 C14 H14 0.9500 C15 C16 1.3900 C15 H15 0.9500 C16 C17 1.3900 C16 H16 0.9500 C17 C18 1.3900	N1 Pd1 N1 78.0(4) N1 Pd1 O1O 176.4(3) N1 Pd1 O1O 98.7(2) N1 Pd1 O2O 100.7(2) N1 Pd1 O2O 178.0(3) O1O Pd1 O2O 82.6(2) N1 Pd1 Pd1 40.12(17) N1 Pd1 Pd1 82.1(2) O1O Pd1 Pd1 138.33(16) O2O Pd1 Pd1 95.89(16) N1 Pd1 Pd1 82.22(19) N1 Pd1 Pd1 40.00(18) O1O Pd1 Pd1 94.29(17) O2O Pd1 Pd1 138.56(15) Pd1 Pd1 Pd1 60.00(6) O1 P1 N1 122.1(2) O1 P1 N1 122.1(2) N1 P1 N1 94.3(3) O1 P1 N1 122.1(2) N1 P1 N1 94.3(3) N1 P1 N1 94.3(3) O1 P1 Pd1 139.48(6) N1 P1 Pd1 47.1(2) N1 P1 Pd1 47.3(2) N1 P1 Pd1 98.4(3) O1 P1 Pd1 139.48(6) N1 P1 Pd1 47.3(2) 4 N1 P1 Pd1 98.4(3) 7 N1 P1 Pd1 47.1(2) Pd1 P1 Pd1 68.48(11) C1O O2O Pd1 112.0(5) C1O O1O Pd1 111.1(5) C11 N1 P1 125.4(5)

	C17 H17 0.9500	C11 N1 Pd1 120.2(5)
	C18 H18 0.9500	P1 N1 Pd1 93.9(3)
		C11 N1 Pd1 117.7(5)
		P1 N1 Pd1 93.7(3)
		Pd1 N1 Pd1 99.9(3)
		O2O C1O O1O 125.9(8)
		O2O C1O C1O 116.4(8)
		O1O C1O C1O 117.6(8)
		C11 C12 H12A 109.5
		C11 C12 H12B 109.5
		H12A C12 H12B 109.5
		C11 C12 H12C 109.5
		H12A C12 H12C 109.5
		H12B C12 H12C 109.5
		N1 C11 C13 110.4(7)
		N1 C11 C12 111.6(7)
		C13 C11 C12 113.4(7)
		N1 C11 H11 107.0
		C13 C11 H11 107.0
		C12 C11 H11 107.0
		C14 C13 C18 120.0
		C14 C13 C11 119.0(5)
		C18 C13 C11 121.0(5)
		C15 C14 C13 120.0
		C15 C14 H14 120.0
		C13 C14 H14 120.0
		C14 C15 C16 120.0
		C14 C15 H15 120.0
		C16 C15 H15 120.0
		C17 C16 C15 120.0
		C17 C16 H16 120.0
		C15 C16 H16 120.0
		C18 C17 C16 120.0
		C18 C17 H17 120.0
		C16 C17 H17 120.0
		C17 C18 C13 120.0
		C17 C18 H18 120.0
		C13 C18 H18 120.0

Characterization data for the ligands

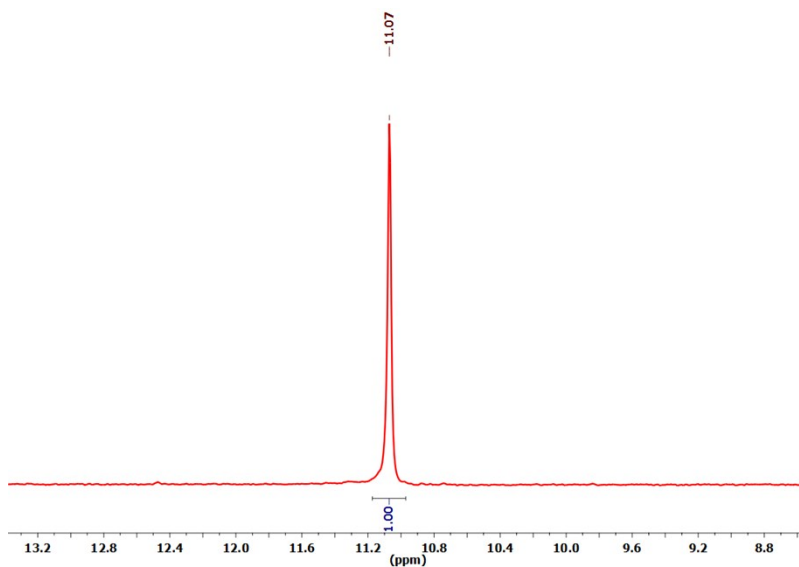


Figure S1. ^{31}P NMR of ligand X^{SH}_3 .

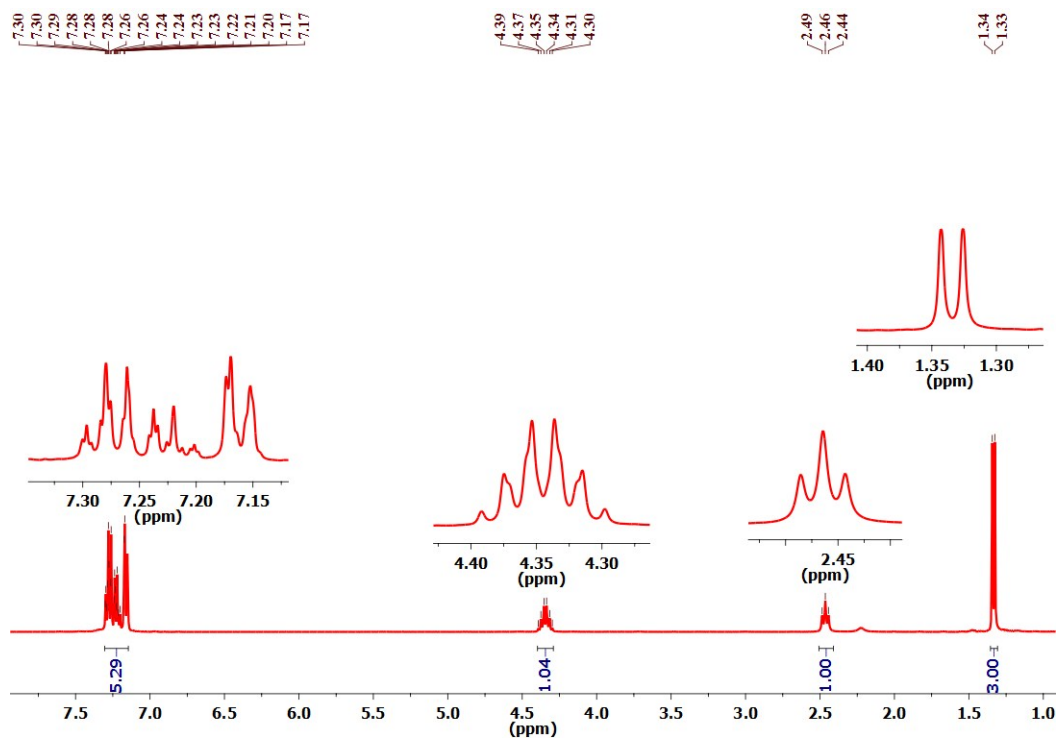


Figure S2. ^1H NMR of ligand X^{SH}_3 .

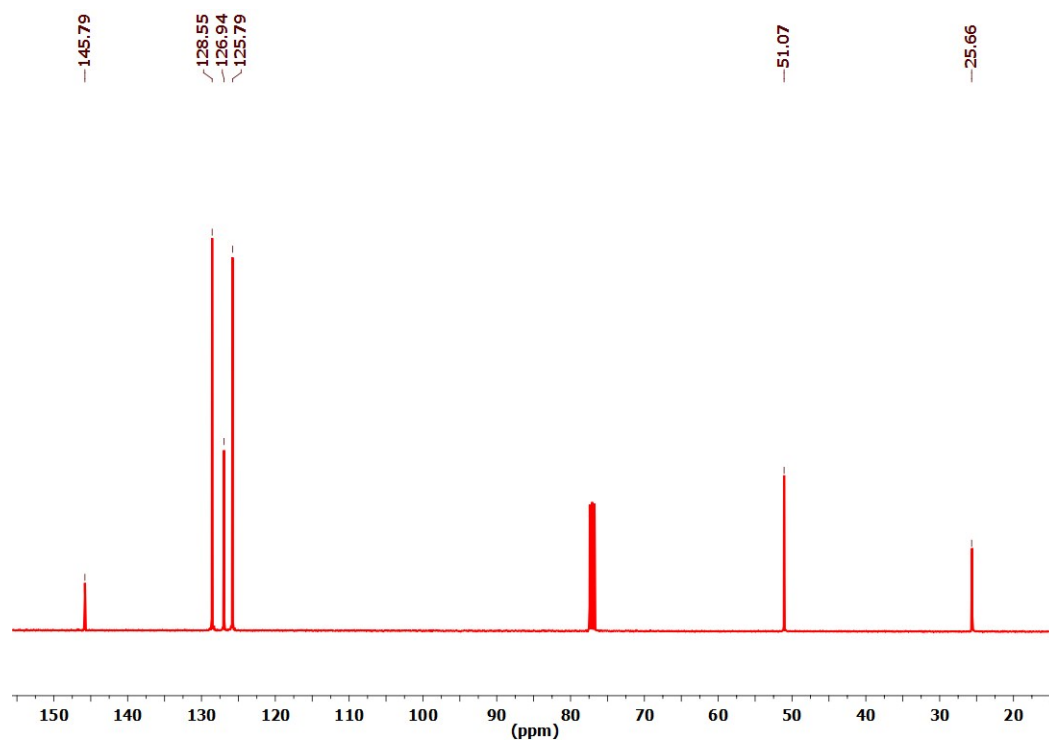


Figure S3. ¹³C NMR of ligand X^SH₃.

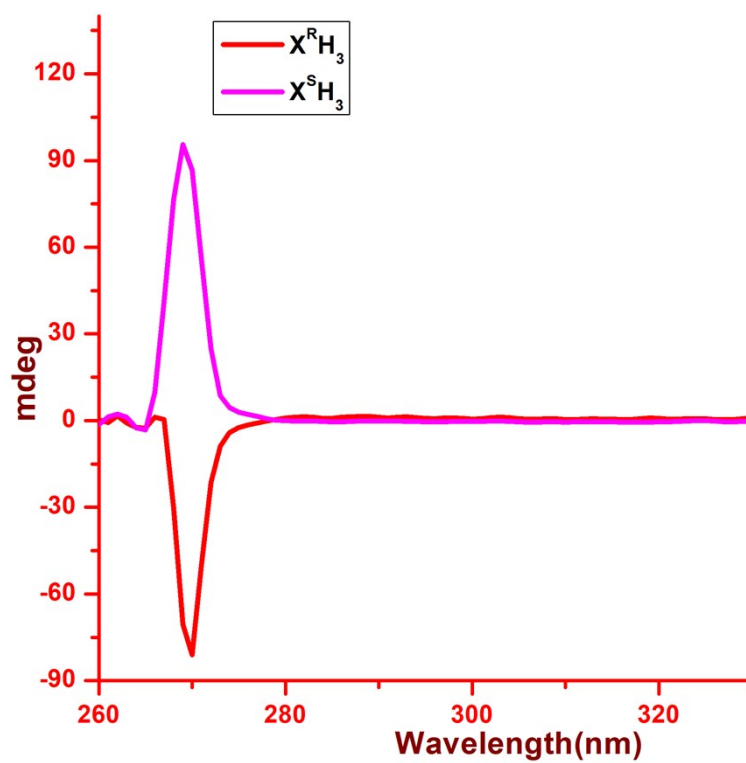


Figure S4. CD spectra of ligands $X^R\text{H}_3$ and $X^S\text{H}_3$ in DCM.

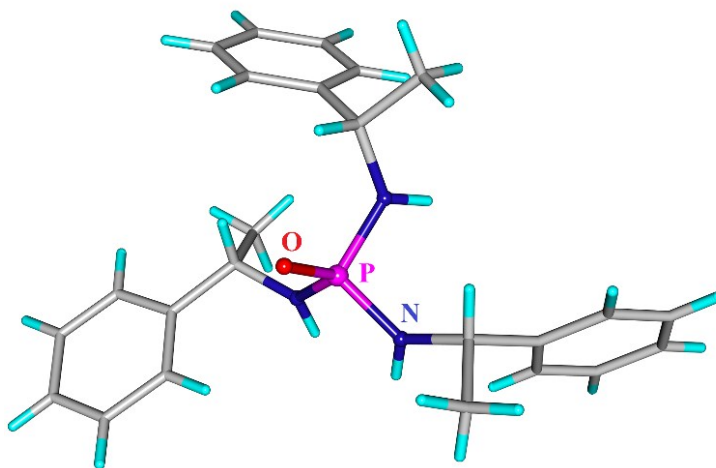


Figure S5. Crystal structures of Ligand $X^S\text{H}_3$.

Spectral data for the chiral tetrahedral cages

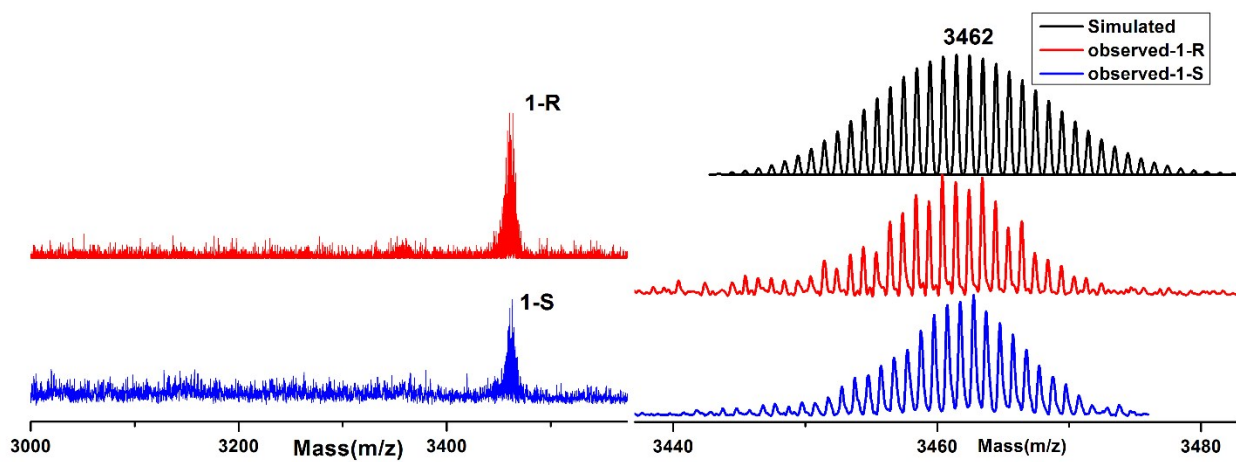


Figure S6. MALDI-TOF mass spectra of **1-R** and **1-S** and their isotopic distribution of peaks.

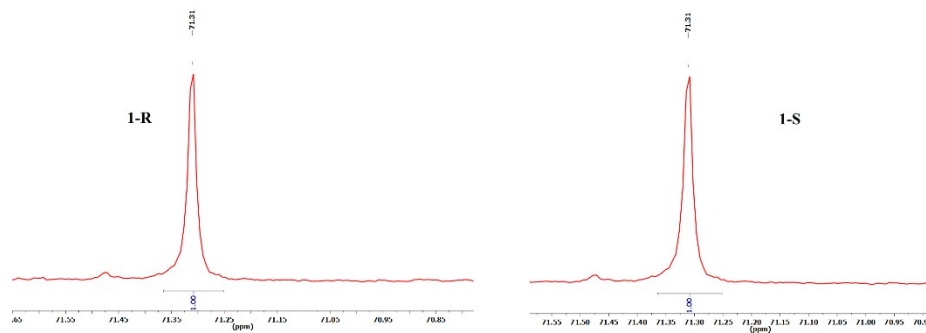


Figure S7. ^{31}P NMR spectra of **1-R** and **1-S**.

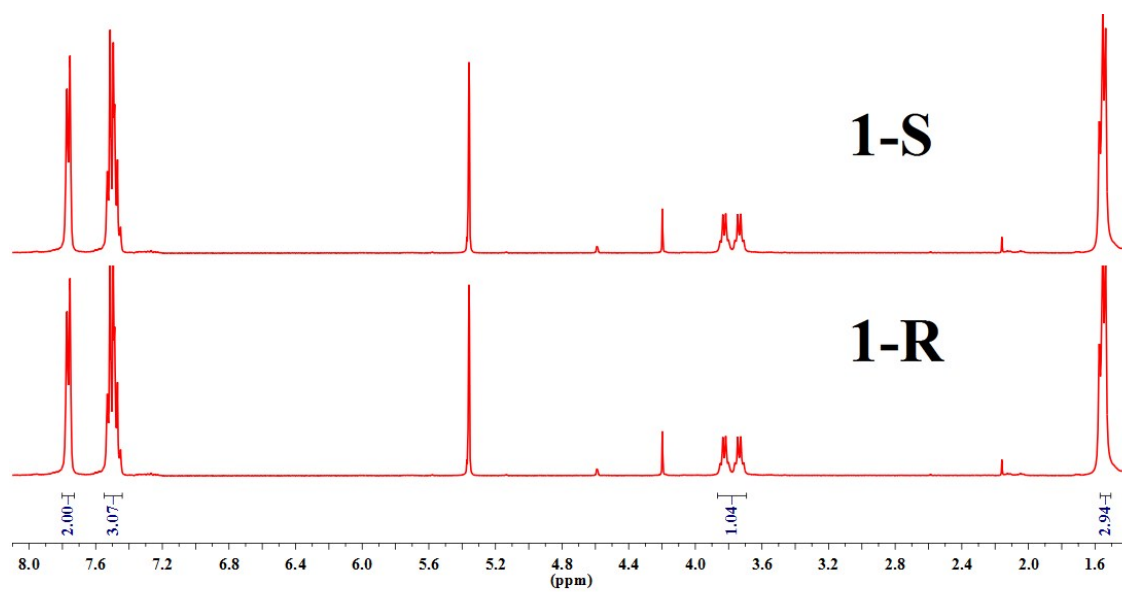


Figure S8. ^1H NMR spectra of **1-R** and **1-S**.

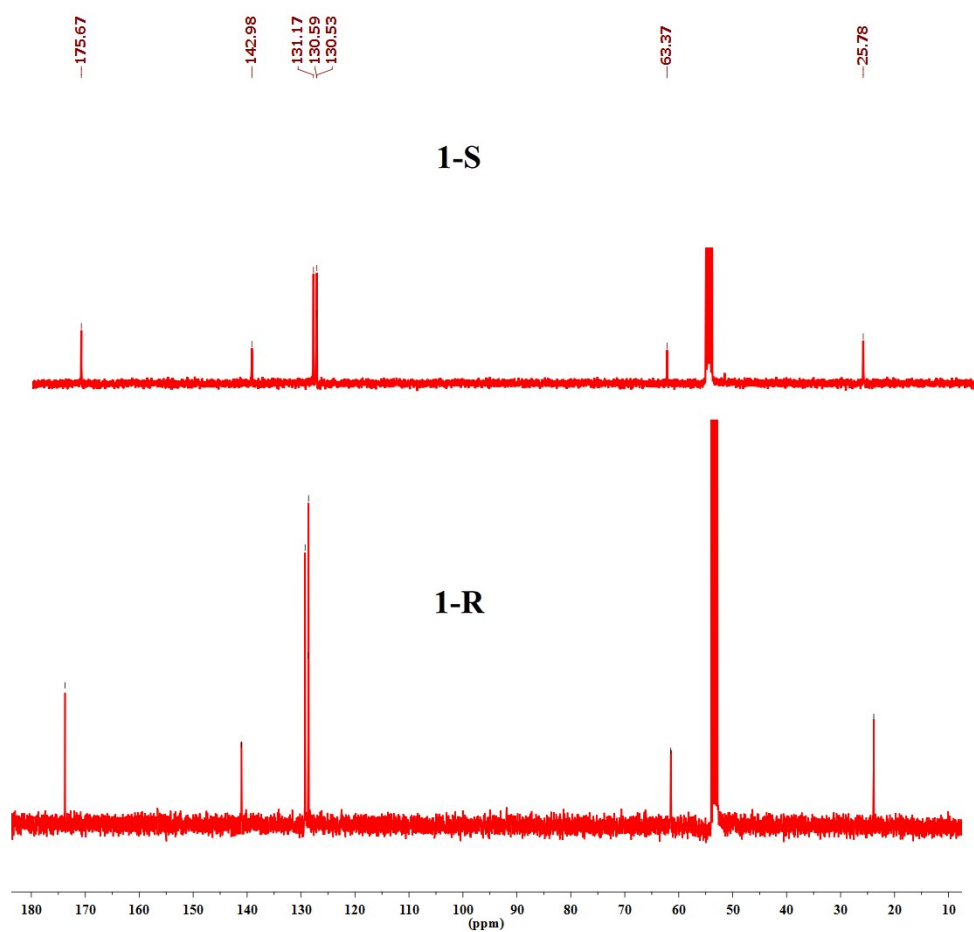


Figure S9. ^{13}C NMR spectra of 1-R and 1-S.

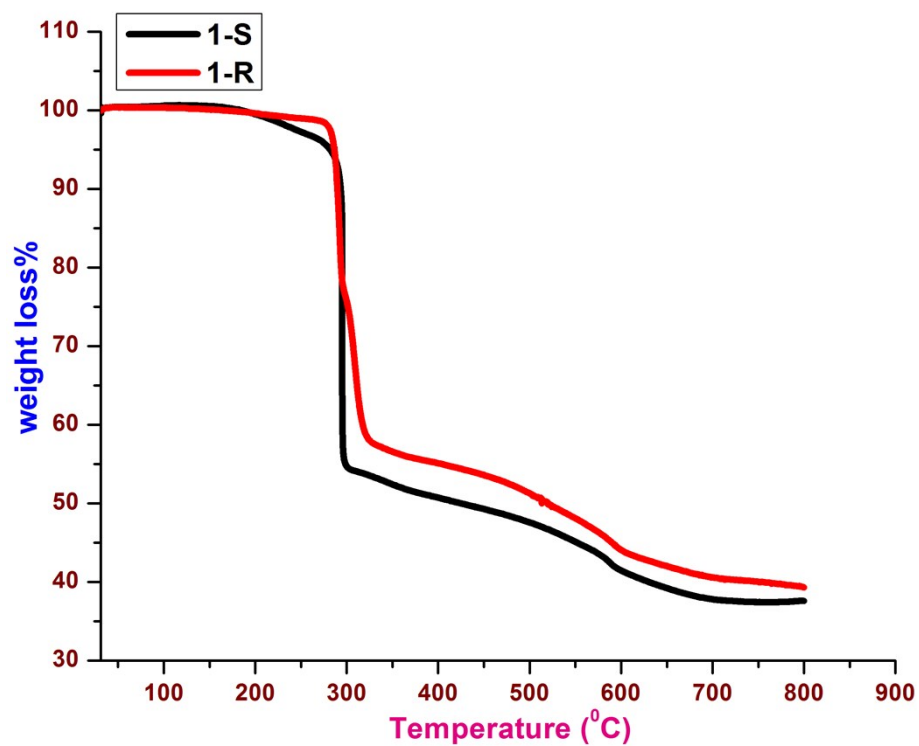


Figure S10. TGA curves of cages 1-R and 1-S.

Structural illustrations and analysis of 1-R and 1-S

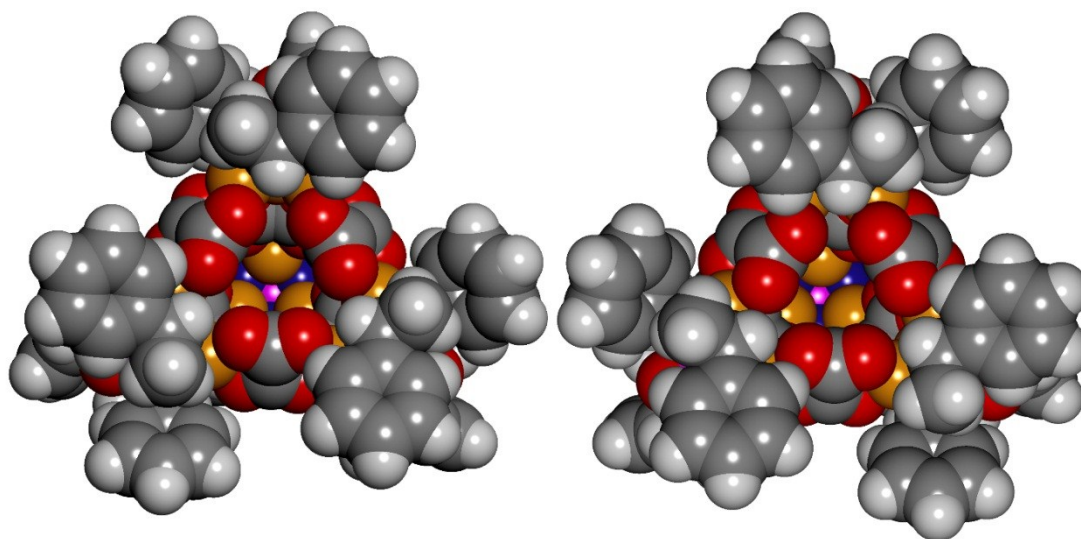


Figure S11.Space-filling view of cage **1-R** and **1-S** showing the definite intrinsic pockets.

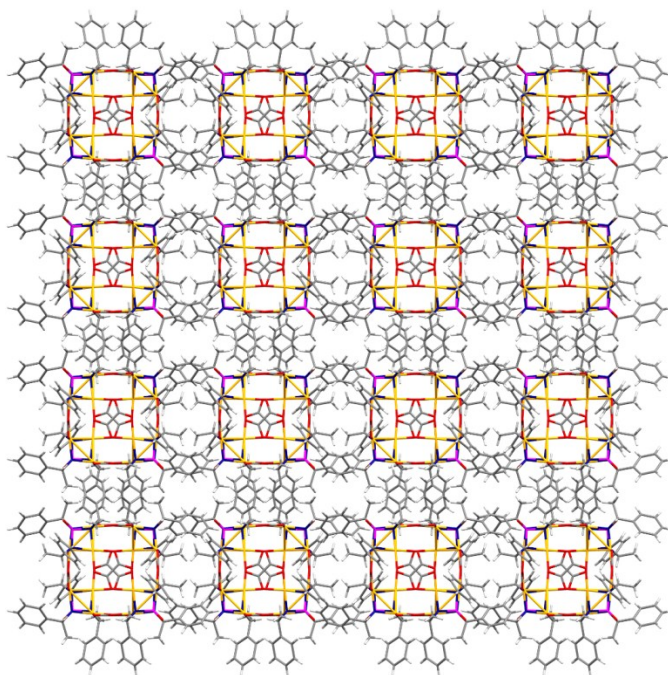


Figure S12. View of packing of the cage **1-R** along the a-axis.

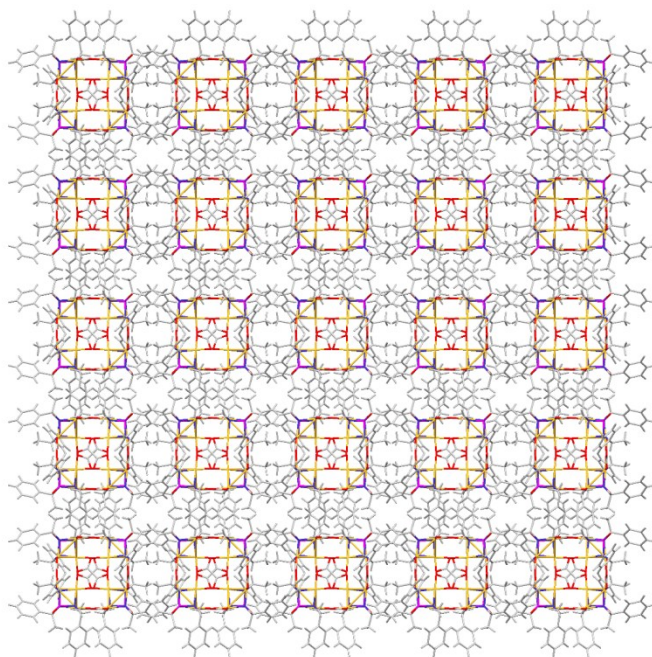


Figure S13. View of packing of the cage **1-S** along the a-axis.

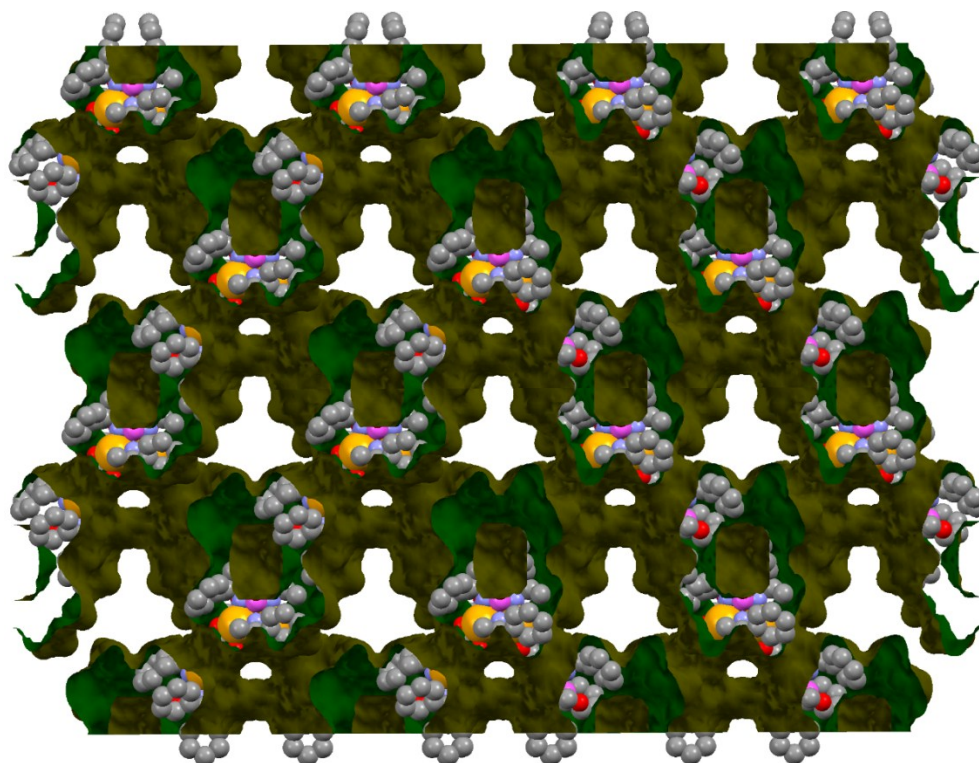


Figure S14. Connolly surface view of the packing structure of **1-S** computed by Mercury software³ showing the location and shape of both the intrinsic (small) and extrinsic (large) cavities.

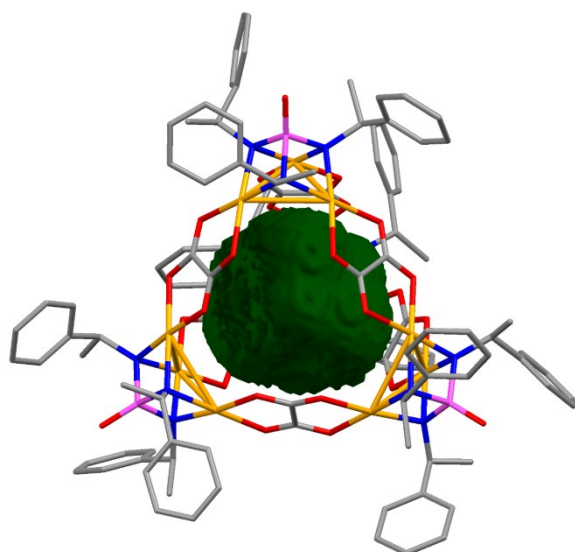


Figure S15. View of the intrinsic cavity surface present in **1-S**.

Table S3: Molecular volume and area calculated for **1-R** from MSROLL calculations⁴

Probe Radius (Å)	Surface Area (Å ²)	Volume (Å ³)
1.3	100.801	86.45
1.4	96.225	83.420
1.5	95.20	79.73

Spectral data for the guest-encapsulated chiral tetrahedral cages

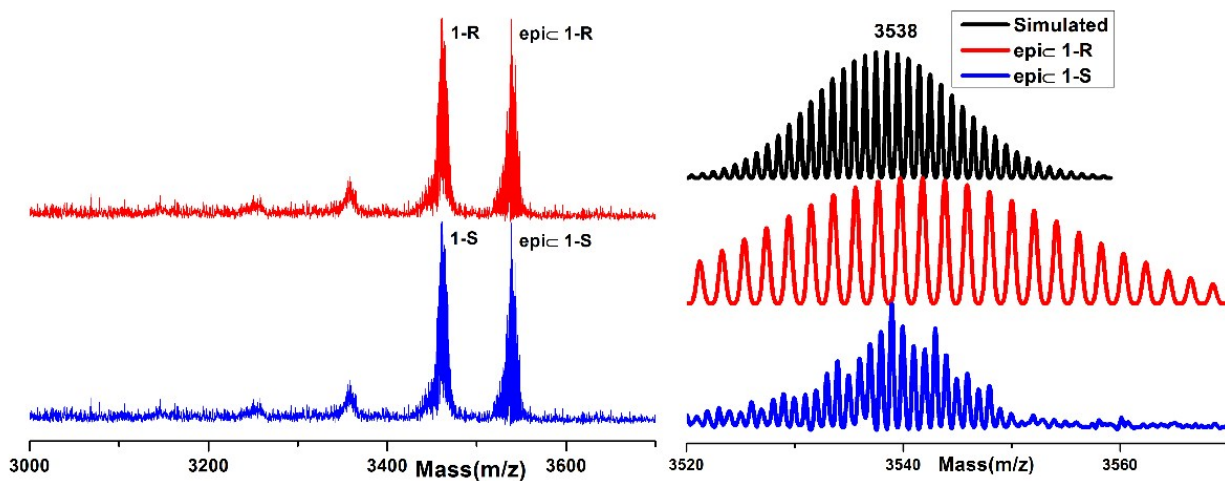


Figure S16. MALDI-TOF spectra of \pm **epic 1-R** and \pm **epic 1-S** and their isotopic distribution of peaks.

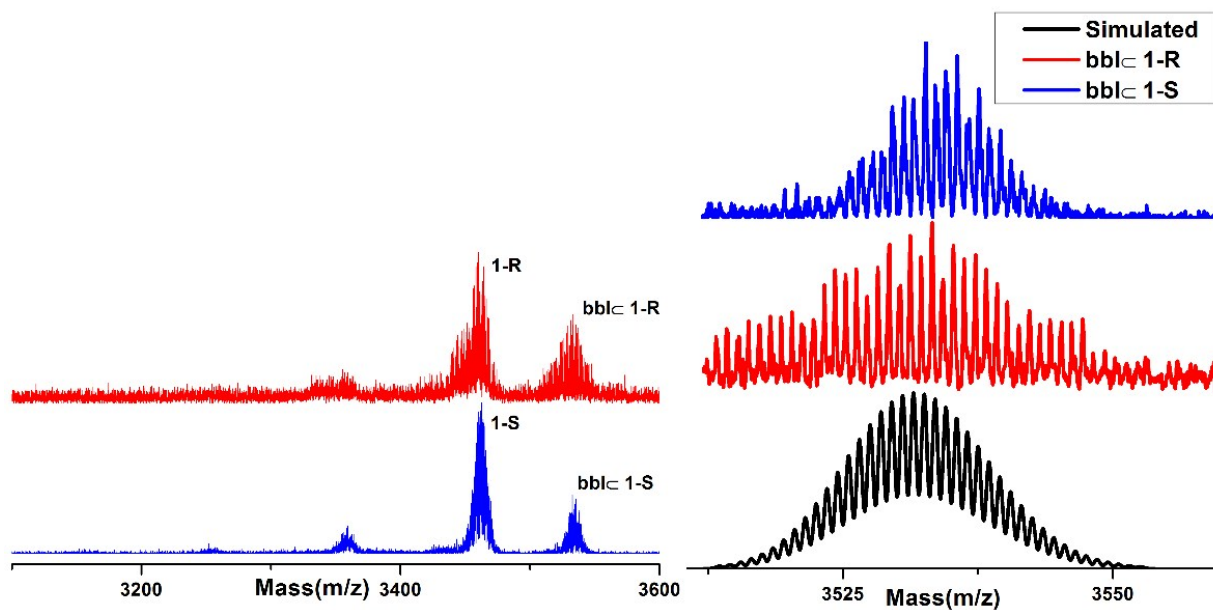


Figure S17. MALDI-TOF spectra of \pm **bbl 1-R** and \pm **bbl 1-S** and their isotopic distribution of peaks.

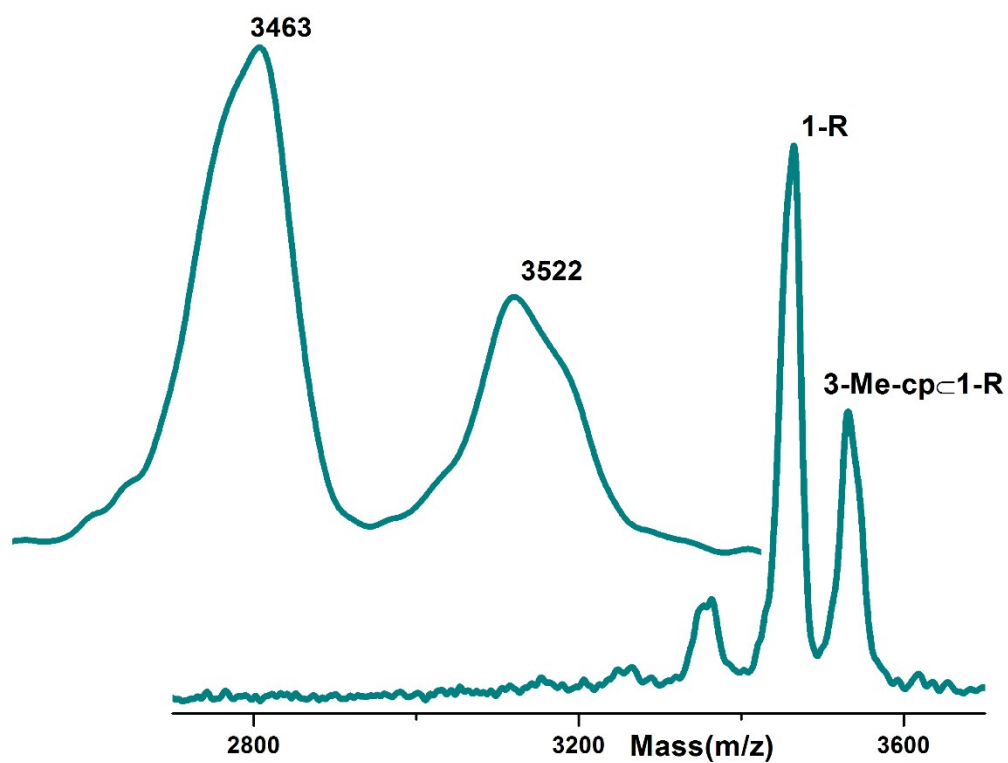


Figure S18. MALDI-TOF spectra of $\pm 3\text{-Me-cp}<1\text{-R}$ in the linear mode.

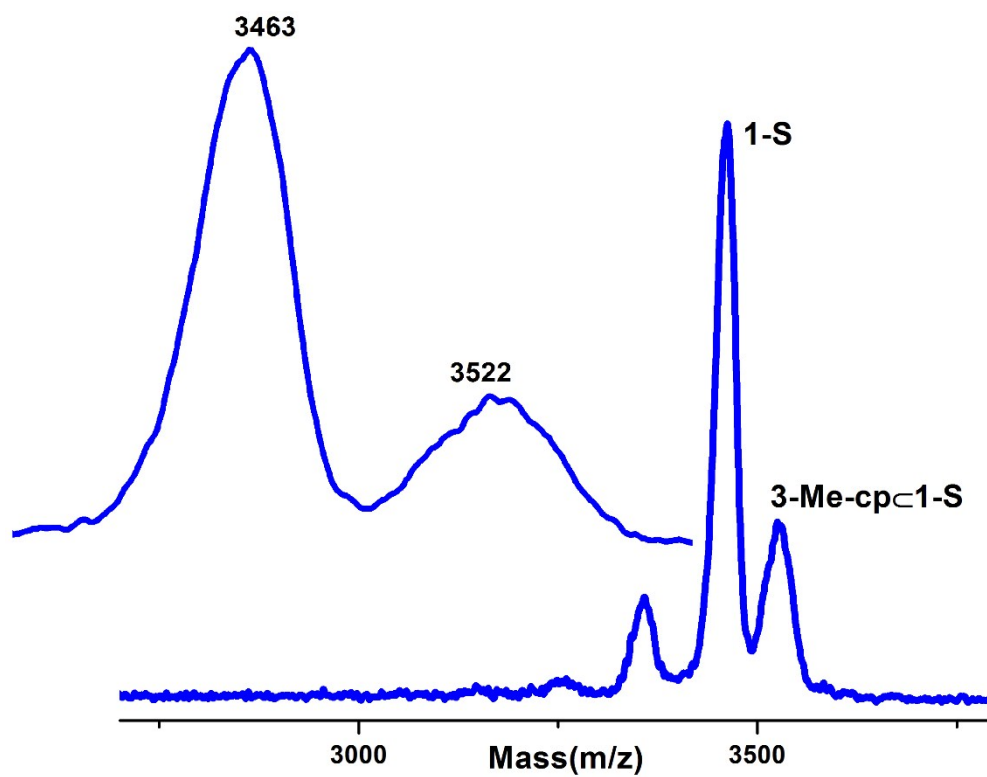


Figure S19. MALDI-TOF spectra of $\pm 3\text{-Me-cp}<1\text{-S}$ in linear mode.

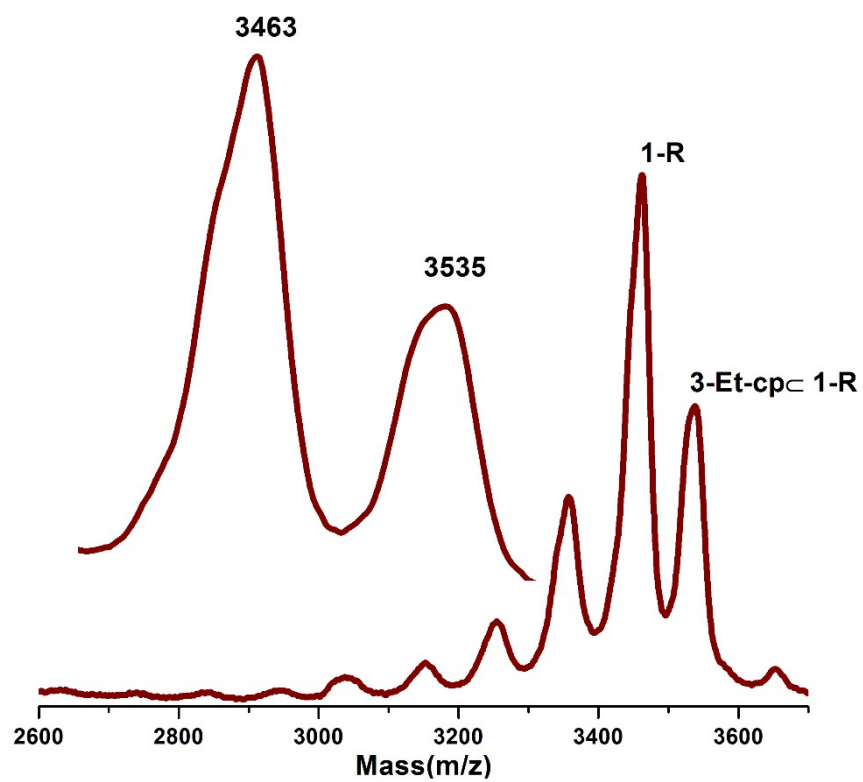


Figure S20. MALDI-TOF spectra of $\pm 3\text{-Et-cp} \subset 1\text{-R}$ in linear mode.

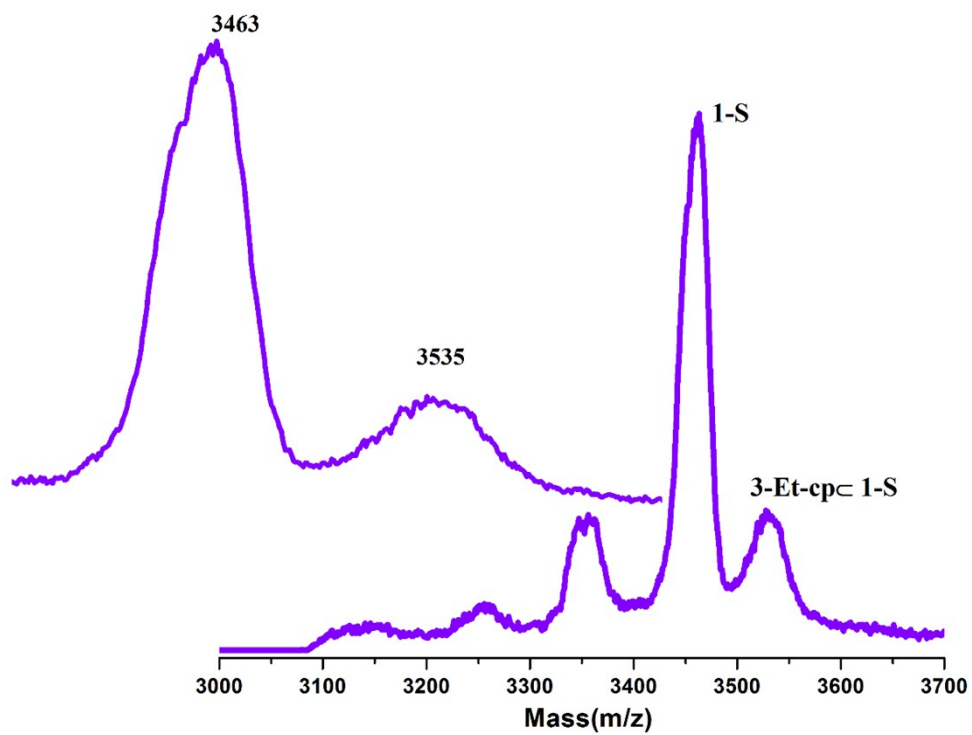


Figure S21. MALDI-TOF spectra of $\pm 3\text{-Et-cp} \subset 1\text{-S}$ in linear mode.

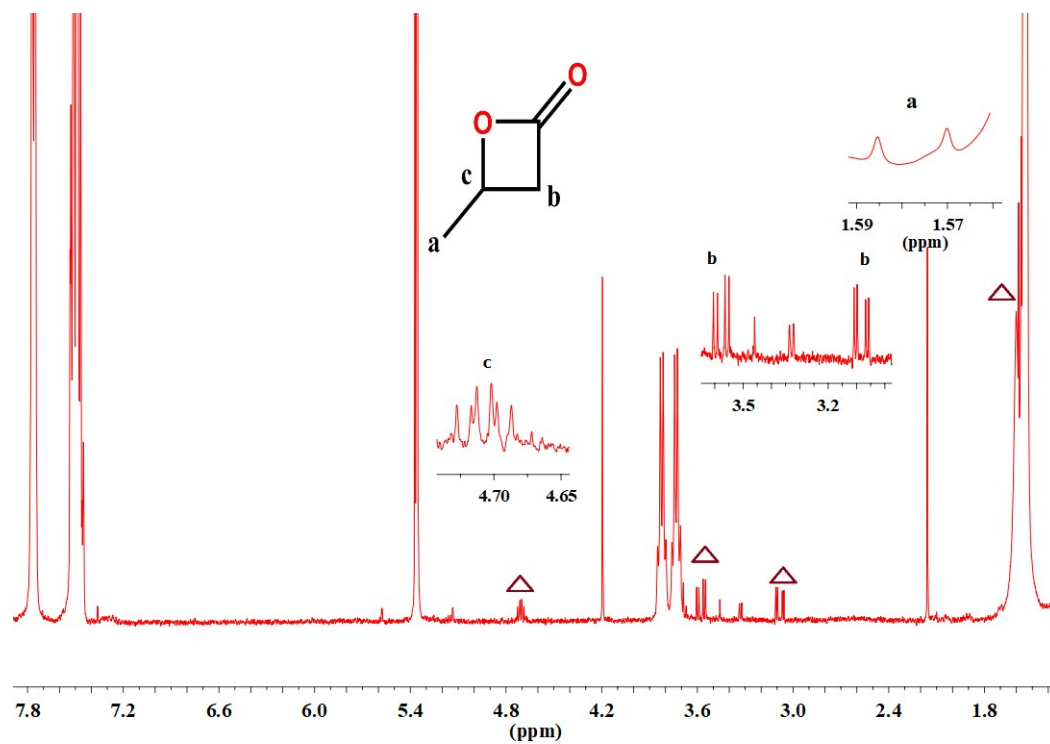


Figure S22. ^1H NMR of **bbl-1-R** and the signals of β -butyrolactone is cartooned by the symbol \triangle .

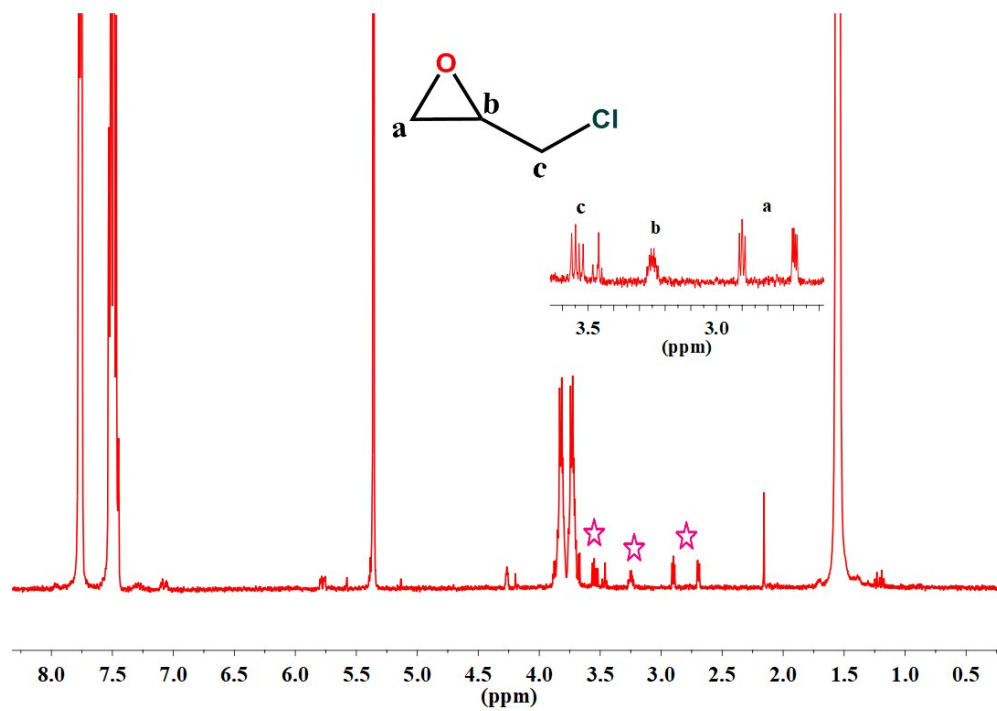


Figure S23. ^1H NMR of **epi-1-R** and the signals of epichlorohydrin is cartooned by \star .

Host-guest NMR Studies:

NMR Diffusion ordered spectroscopy (DOSY) experiments were performed on Bruker AVANCE III 600MHz NMR at constant temperature of 298 K. The samples were prepared by dissolving 5 mg of 1-R (or 1-S) in 500 μ l CD₂Cl₂ (Sigma Aldrich). The guest molecules were added individually to host and allowed to equilibrate for 12 hr (unless otherwise specified) before data acquisition. Diffusion ordered spectroscopy (DOSY) experiments were performed by varying gradient strength between 2-95%. Diffusion time (Δ) and length of the gradient (δ) was optimized for each host-guest system so as to get ~90-95 % signal attenuation in host and guest peak individually at 95 % gradient strength. 32 Data points were collected between 2-95 % of gradient strength with 16 scans for each gradient step. Data collected was processed using standard Bruker protocol with SimFit algorithm as described elsewhere.⁵ The Fitting of the diffusion data was done in OriginPro 8.5.0 using equation 1 for single diffusion coefficient and equation 2 for the bimodal decay with two diffusion coefficients.

$$I = I_0 \exp \left[-D\gamma^2 g^2 \delta^2 \left(\Delta - \frac{\delta}{3} \right) \right] \quad (1)$$

$$I = I_{0A} \exp \left[-D_A \gamma^2 g^2 \delta^2 \left(\Delta - \frac{\delta}{3} \right) \right] + I_{0B} \exp \left[-D_B \gamma^2 g^2 \delta^2 \left(\Delta - \frac{\delta}{3} \right) \right] \quad (2)$$

where, I is the observed integral, I_0 (I_{0A} and I_{0B} for equation 2) the reference or un-attenuated integral, D (D_A and D_B for equation 2) the diffusion coefficient(s), γ the gyromagnetic magnetic ratio of the observed nucleus, g the gradient strength, δ the length of gradient pulse and Δ the diffusion time. Intensity decay data, however, failed to fit to equation 2.

A single diffusion coefficient was obtained from the DOSY analysis for all the data sets for either the host peak or the guest peak (Figure S23).¹² Diffusion coefficients (D) for guests were dispersed between 21.34 and 28.99 $\times 10^{-9}$ m²/s while for hosts it ranged from 13.57 to 20.02 $\times 10^{-9}$ m²/s. To test whether the encapsulation of guest in host is concentration dependent, for (\pm)bbl and (\pm)3-Et-cp, DOSY experiments were performed by adding 1, 10 and 24 equivalents of guest to the host. To test delayed encapsulation of the guest in host, (\pm)bbl in 1:1 host-guest system was tested after 120 hr. Diffusion coefficient for host-guest conditions were measured for hosts (1-R and 1-S) and various guests as mentioned in table S3.

From these data, it can be noted that for each host-guest condition, difference in diffusion coefficient values for the corresponding host and guest is c.a. $8.42 \pm 0.03 \times 10^{-9}$ m²/s. This means that guests are diffusing only slightly faster than hosts and by a similar factor irrespective of the nature of host/concentration/incubation time suggestive of some sort of interaction between them. Also, it suggests that guests are not firmly bound to hosts at their intrinsic cavities but are loosely associated with them at the chiral exteriors under the solution conditions. Further, from the DOSY data obtained on enantiopure epi molecules (+epi and -epi) no selective chiral recognition was observed as evident from the similar D -values for all the four scenarios probed (+epi \subset 1-R, +epi \subset 1-S, -epi \subset 1-R and -epi \subset 1-S).

Table S3: Diffusion coefficients for the various host-guest systems studied

System No.	Host- Guest system	Equivalents of Guest	Diffusion coefficient (*1E ⁻⁹ m ² /s)	
			Host peak	Guest peak
1	R(-)epi \subset 1-R	10	20.02 \pm 0.26	28.99 \pm 0.16
2	S(+epi \subset 1-S	10	17.77 \pm 0.10	27.56 \pm 0.13
3	R(-)epi \subset 1-S	10	16.08 \pm 0.12	23.22 \pm 0.10
4	S(+epi \subset 1-R	10	18.87 \pm 0.19	28.82 \pm 0.16

5	(\pm)bbl \subset 1-R	1	13.57 ± 0.08	22.06 ± 0.08
6	(\pm)bbl \subset 1-R*	1	18.16 ± 0.15	26.01 ± 0.11
7	(\pm)bbl \subset 1-R	10	17.94 ± 0.23	26.83 ± 0.13
8	(\pm)bbl \subset 1-R	24	15.99 ± 0.12	23.37 ± 0.08
9	(\pm)3-Et-cp \subset 1-R	1	16.40 ± 0.08	24.71 ± 0.09
10	(\pm)3-Et-cp \subset 1-R	10	13.80 ± 0.07	21.34 ± 0.07
11	(\pm)3-Et-cp \subset 1-R	24	19.58 ± 0.17	27.92 ± 0.12

System marked with () was incubated for 120 hr.

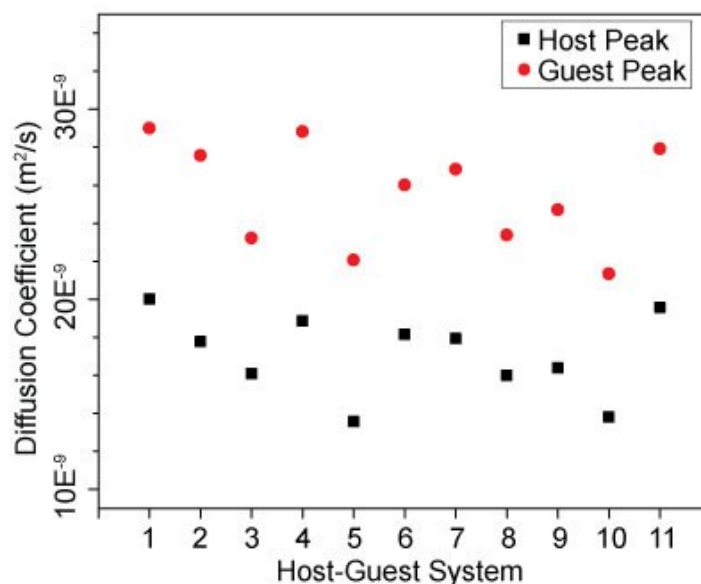


Figure S24. Summary of diffusion coefficients obtained for different host guest systems. The systems are numbered as mentioned in table S3.

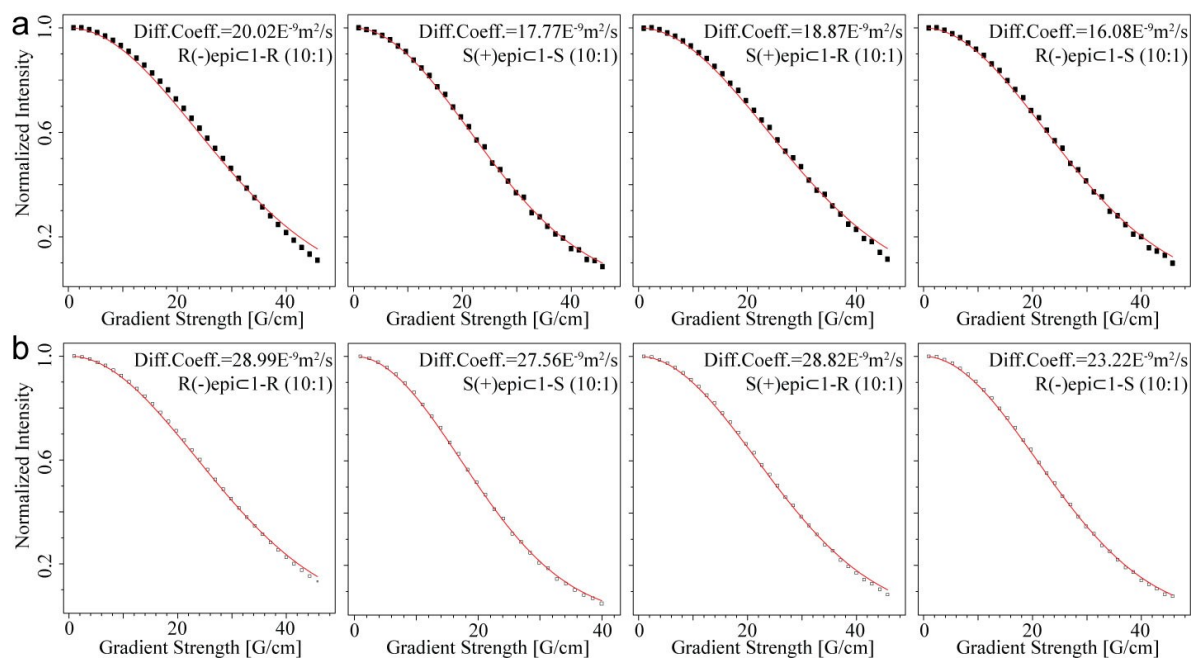


Figure S25. Integral decay profile of (a) host protons (filled box) and (b) guest protons (open box) for epi \subset host systems.

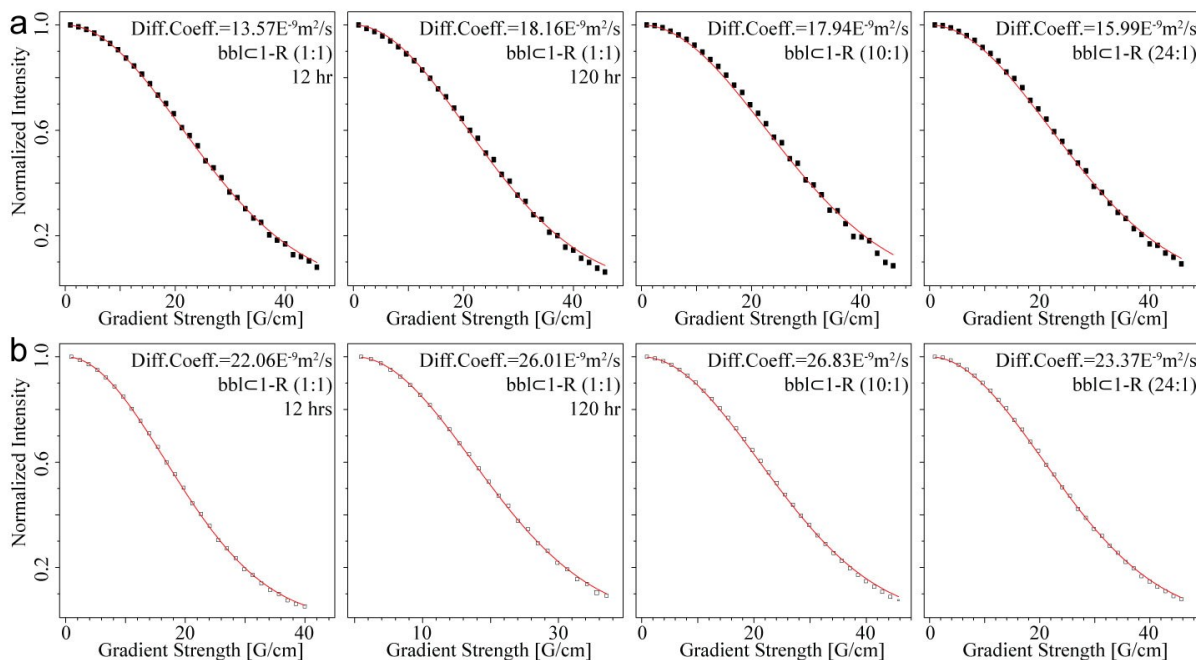


Figure S26. Integral decay profile of (a) host protons (filled box) and (b) guest protons (open box) for (\pm)bbl \subset host systems.

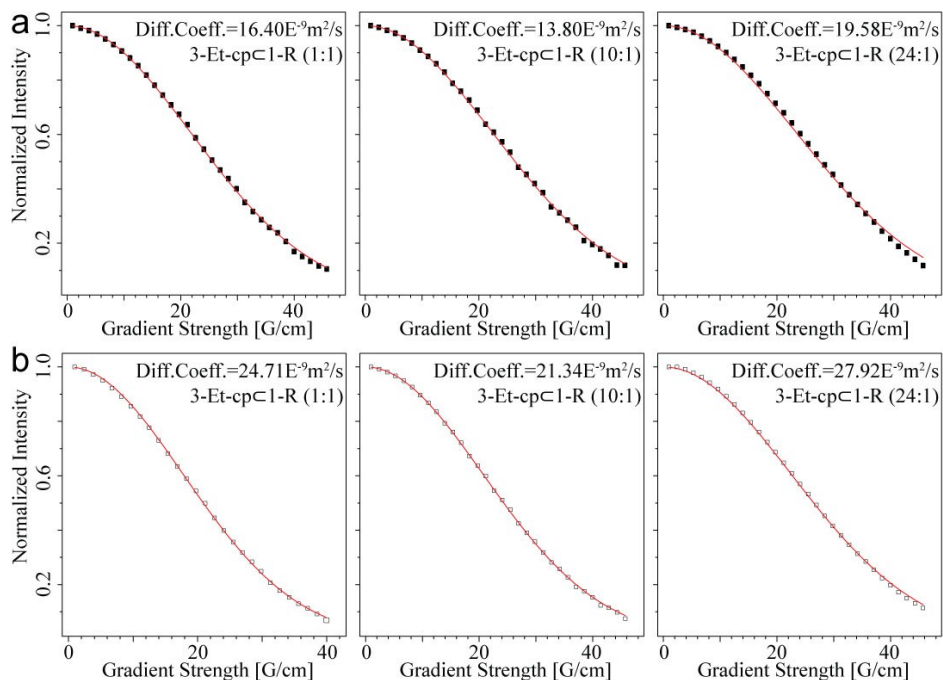


Figure S27. Integral decay profile of (a) host protons (filled box) and (b) guest protons (open box) for (\pm) 3-Et-cp \subset host systems

Structural illustrations of $\pm\text{bbl}\subset\pm\mathbf{1}$

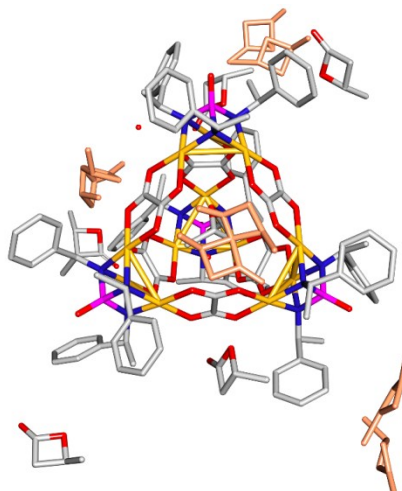


Figure S28. Molecular structure of $\pm\text{bbl}\subset\pm\mathbf{1}$ with disordered bbl guest molecules shown in light orange colour

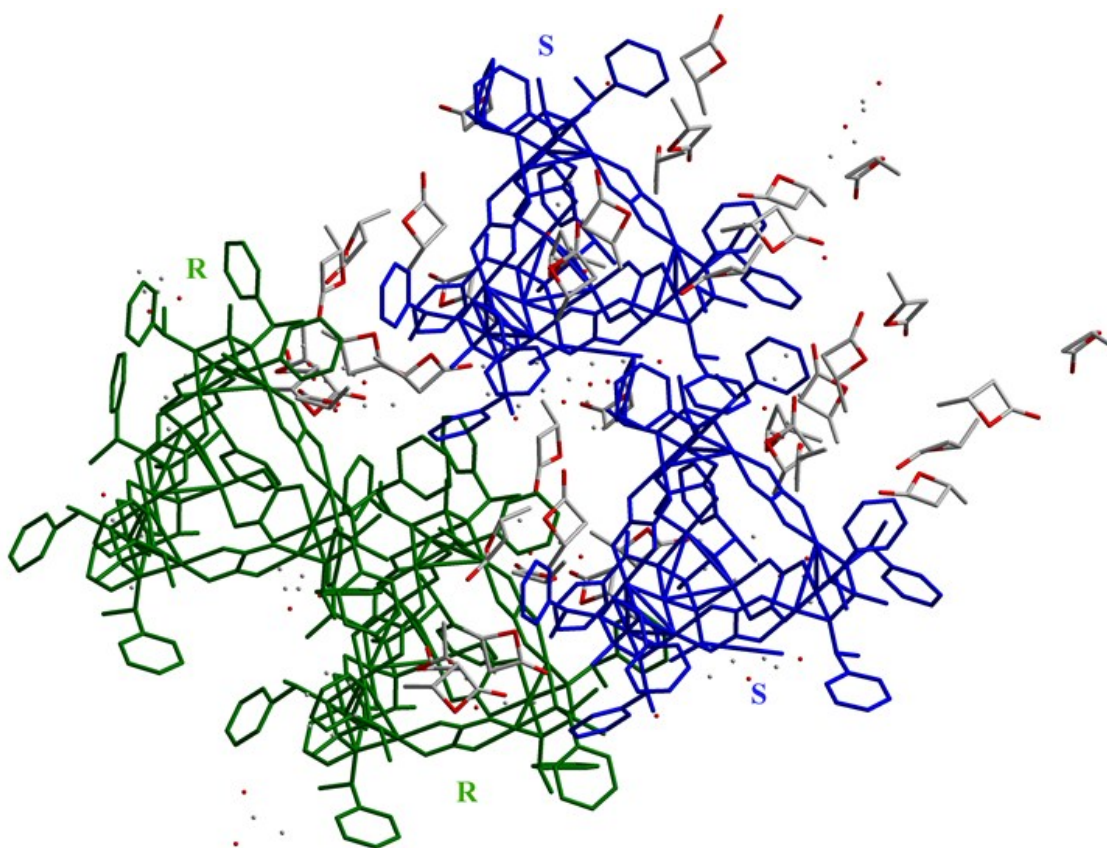


Figure S29. 2x2x2 packing structure of $\pm\text{bbl}\subset\pm\mathbf{1}$ showing both location of bbl guests at the intrinsic (green colour) and extrinsic cavities orders (blue) and disordered (orange).

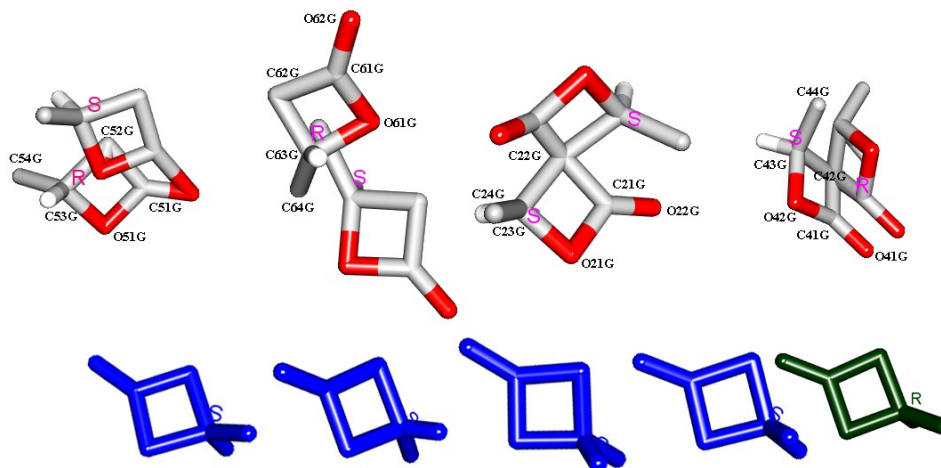


Figure S30. $\pm bbl \subset \pm 1$ showing both disordered (top) and ordered bbl (bottom) guests present in the extrinsic cavities: S-bbl shown in blue and R-bbl shown in green.

Low Pressure Gas Sorption Studies

Low pressure CO₂ gas sorption measurements were performed using Micromeritics 3-Flex surface area and porosimetry analyzer. All the gasses used were of high purity (99.9999%). To get all isotherms, about 100 mg of the sample was activated by heating the sample at 50°C under vacuum for 6 hours and was directly loaded to the analysis port. The pore size distribution was calculated from 195K CO₂ isotherm using DFT model.

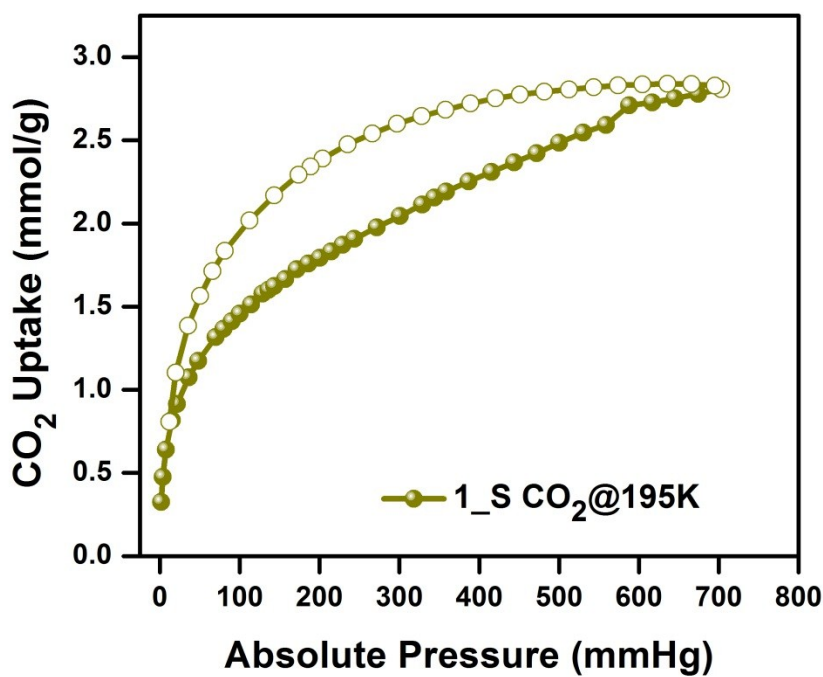


Figure S31. CO₂ Adsorption (solid spheres) and desorption profile (hollow spheres) for 1-S at 195K.

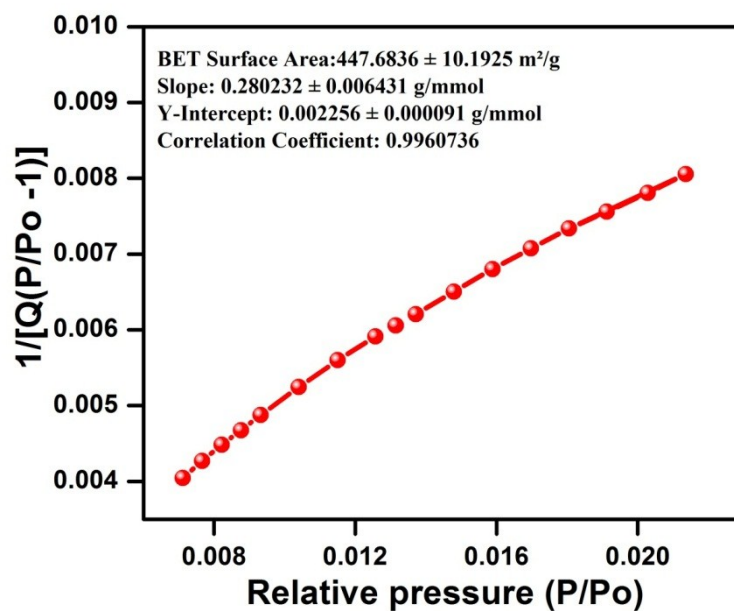


Figure S32. BET surface area for 1-S obtained from the 195K CO₂ adsorption data.

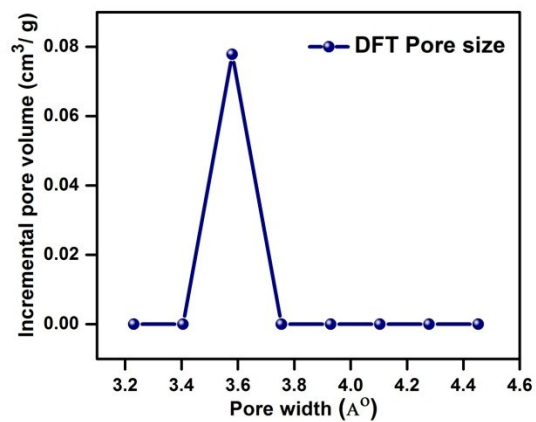


Figure S33. DFT derived Pore size distribution plot for 1-S calculated from the 195K CO₂ adsorption data.

GC Methods for the Enantiomeric Separation of the Chiral Guest Molecules

Table S4: Summary of GC-separation results for the racemic guest molecules by **1-R** and **1-S**.

Guest Substrate	Resolved <i>ee</i> by 1-R (%)	Resolved <i>ee</i> by 1-S (%)
epichlorohydrin	6	10
β -butyrolactone	34	14
3-Me-cyclopentanone	14	16
3-Et-cyclopentanone	12	14

1. Enantiomeric separation of epichlorohydrin

Column used: Supelco γ -dex (30 m* 0.25 mm * 0.25 μ m),

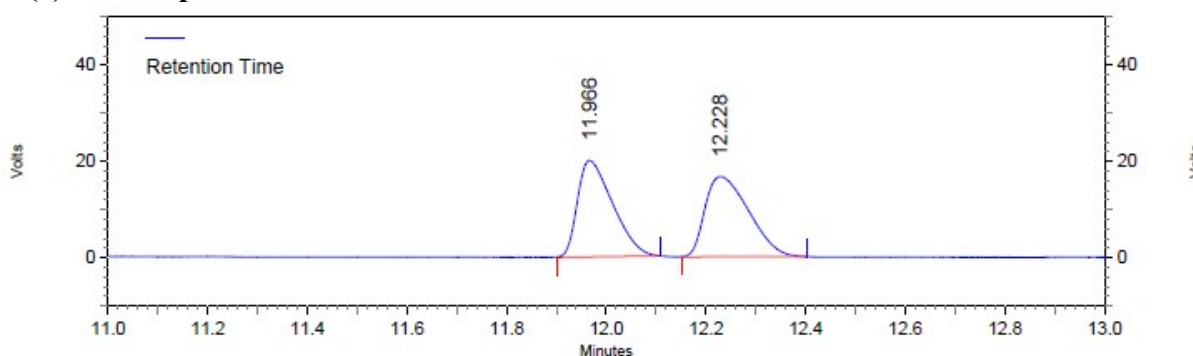
Split ratio 30:1,

Inlet temperature 210 $^{\circ}$ C,

Column pressure 7 psi,

Temperature programme: started at 50 $^{\circ}$ C, hold for 2 mins then heated at rate of 10 $^{\circ}$ C to 100 $^{\circ}$ C followed by heating at rate of 2 $^{\circ}$ C to 160 $^{\circ}$ C. Finally it was heated at the rate of 10 $^{\circ}$ C to Maximum temperature (210 $^{\circ}$ C).

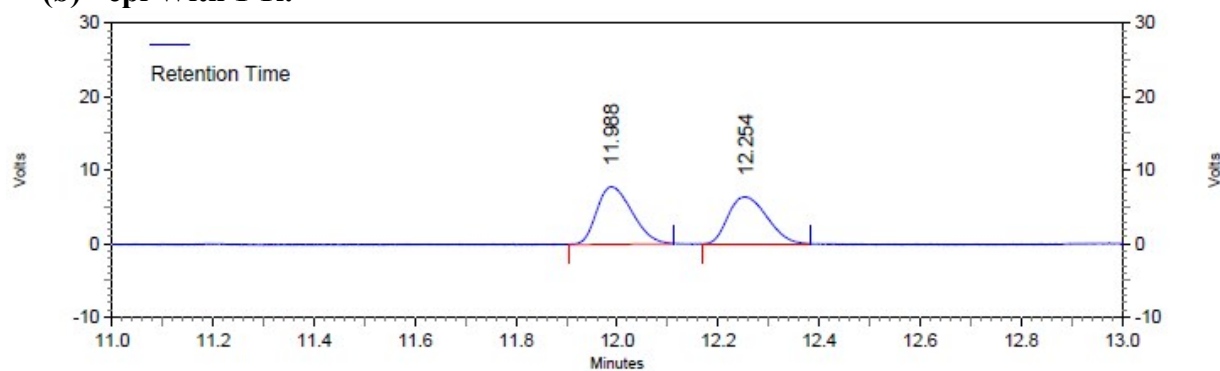
(a) Neat \pm epi:



Front Signal Results				
Retention Time	Area	Area %	Height	Height %
11.966	755741	49.20	154033	54.60
12.228	780432	50.80	128089	45.40
Totals	1536173	100.00	282122	100.00

Figure S34. GC chromatogram and analysis plot showing the resolved peaks for rac-epichlorohydrin

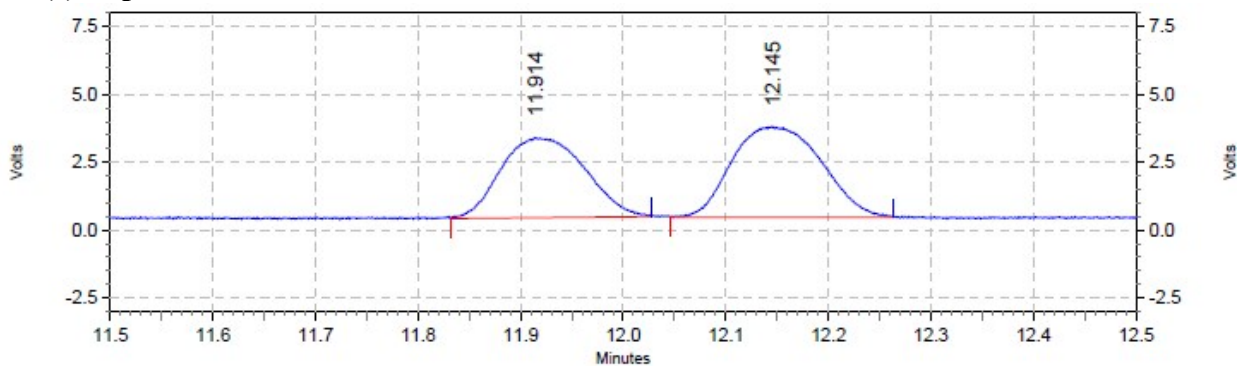
(b) \pm epi With 1-R:



Front Signal Results				
Retention Time	Area	Area %	Height	Height %
11.988	292035	52.44	60034	54.89
12.254	264833	47.56	49343	45.11
Totals	556868	100.00	109377	100.00

Figure S35. GC chromatogram and analysis plot for the resolved peaks of epichlorohydrin extracted from 1-R cage showing 6% *ee*.

(c) \pm epi With 1-S:



Front Signal Results				
Retention Time	Area	Area %	Height	Height %
11.914	128946	45.22	22729	46.84
12.145	156231	54.78	25799	53.16
Totals	285177	100.00	48528	100.00

Figure S36. GC chromatogram and analysis plot for the resolved peaks of epichlorohydrin extracted from 1-S cage showing 10% *ee*.

2. Enantiomeric separation of β -butyrolactone:

Column used: Supelco β -dex (30 m* 0.25 mm * 0.25 μ m),

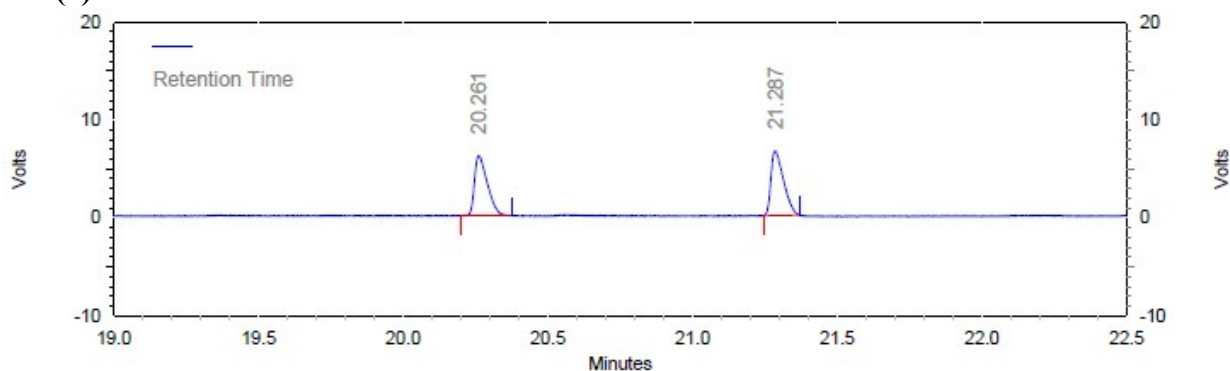
Split ratio 30:1,

Inlet temperature 210 $^{\circ}$ C,

Column pressure 15.1 psi

Temperature programme: started at 80 $^{\circ}$ C, hold for 1 mins then heated at the rate of 4 $^{\circ}$ C to 160 $^{\circ}$ C. Finally heated at the rate of 10 $^{\circ}$ C to 210 $^{\circ}$ C and hold for 2 mins

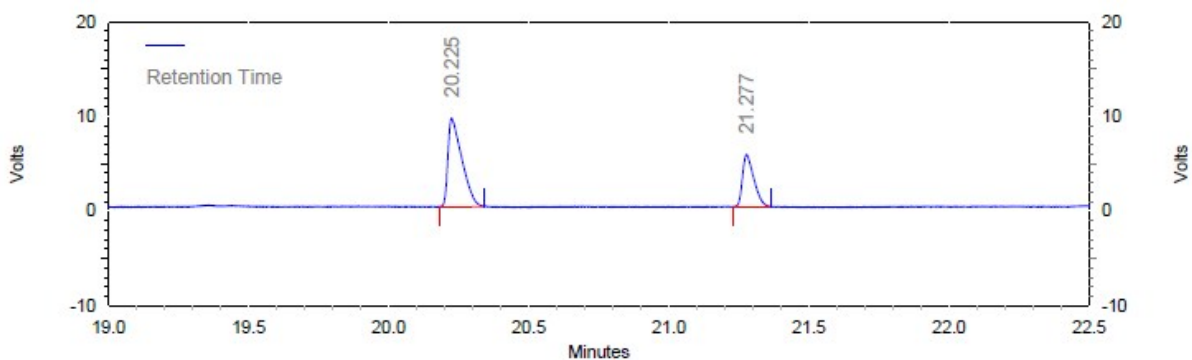
(a) Neat \pm bbl:



Front Signal Results				
Retention Time	Area	Area %	Height	Height %
20.261	147976	49.13	47414	48.30
21.287	153187	50.87	50753	51.70
Totals				
	301163	100.00	98167	100.00

Figure S37. GC chromatogram and analysis plot showing the resolved peaks for rac- β -butyrolactone.

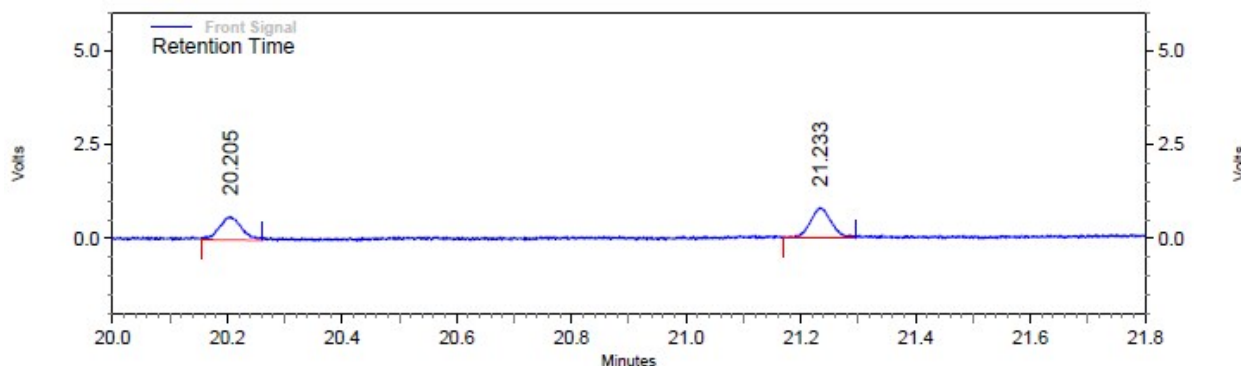
(b) \pm bbl with 1-R:



Front Signal Results				
Retention Time	Area	Area %	Height	Height %
20.225	249952	67.23	72382	62.89
21.277	121844	32.77	42709	37.11
Totals	371796	100.00	115091	100.00

Figure S38. GC chromatogram and analysis plot for the resolved peaks of bbl extracted from **1-R** cage showing 34% *ee*.

(c) \pm bbl with 1-S:



Front Signal Results				
Retention Time	Area	Area %	Height	Height %
20.205	12749	43.38	4830	43.21
21.233	16643	56.62	6349	56.79
Totals	29392	100.00	11179	100.00

Figure S39. GC chromatogram and analysis plot for the resolved peaks of bbl extracted from **1-S** cage showing 14% *ee*.

3. Enantiomeric separation of 3-methylcyclopentanone:

Column used: Supelco β -dex (30 m* 0.25 mm * 0.25 μ m),

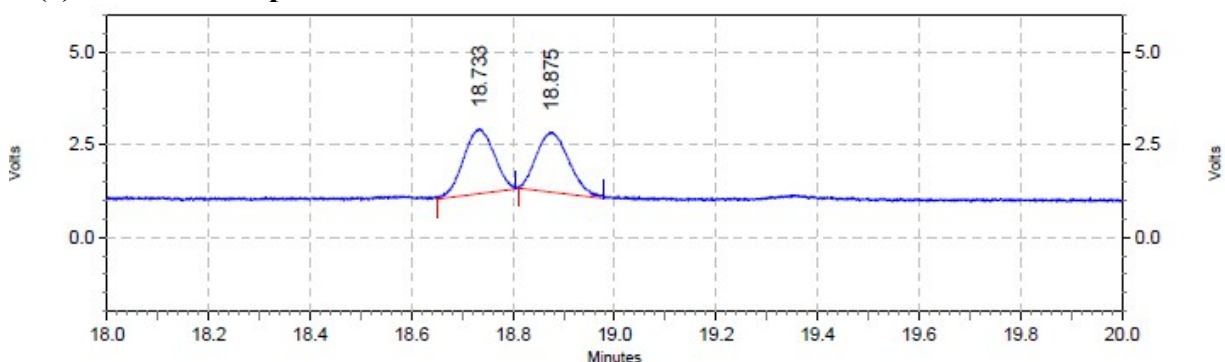
Split ratio 30:1,

Inlet temperature 210 $^{\circ}$ C,

Column pressure 7 psi

Temperature programme: started at 50 $^{\circ}$ C, then ramped at the rate of 10 $^{\circ}$ C to 90 $^{\circ}$ C then heated at the rate of 3 $^{\circ}$ C to 130 $^{\circ}$ C hold for 3 mins It was further heated at the rate of 2 $^{\circ}$ C to 150 $^{\circ}$ C.Finally heated at the rate of 10 $^{\circ}$ C to 210 $^{\circ}$ C

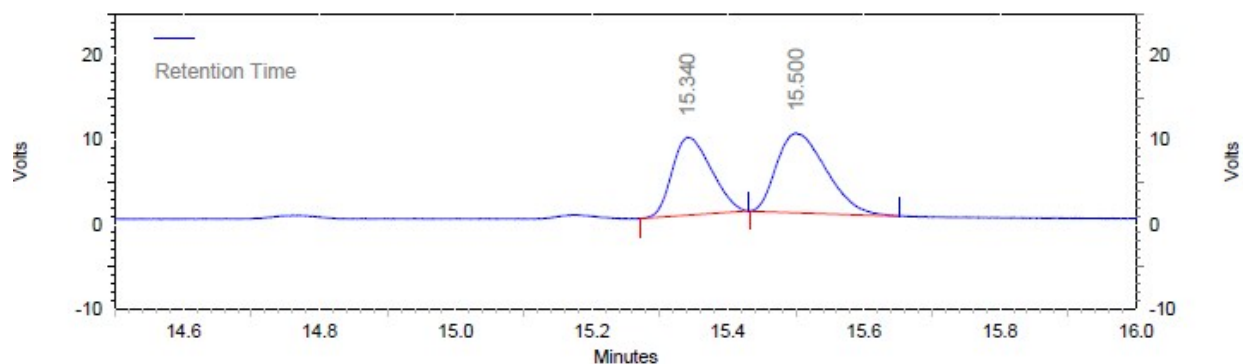
(a) Neat \pm 3-Me-cp:



Front Signal Results				
Retention Time	Area	Area %	Height	Height %
18.733	56507	50.43	13506	51.94
18.875	55535	49.57	12495	48.06
Totals	112042	100.00	26001	100.00

Figure S40. GC chromatogram and analysis plot showing the resolved peaks for rac-3-methylcyclopentanone

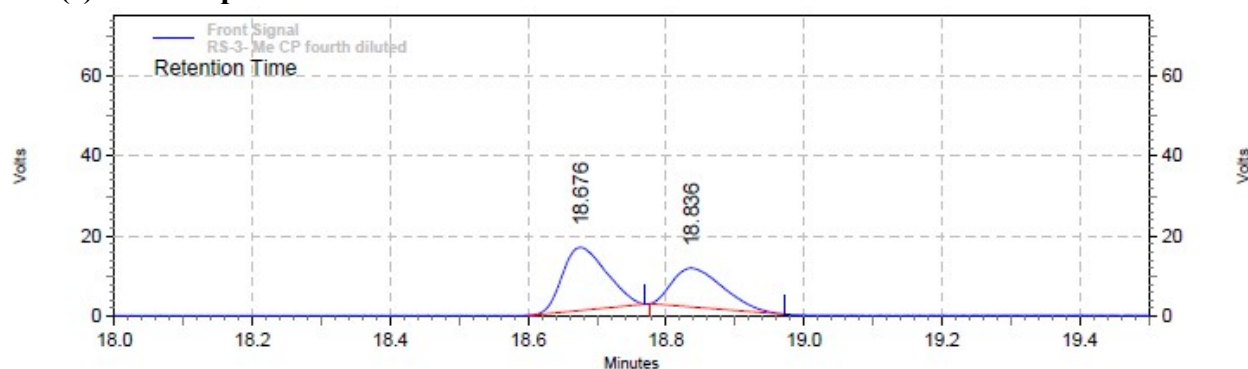
(b) \pm 3-Me-cp with 1-R:



Front Signal Results				
Retention Time	Area	Area %	Height	Height %
15.340	283033	43.51	71050	49.41
15.500	367454	56.49	72752	50.59
Totals	650487	100.00	143802	100.00

Figure S41. GC chromatogram and analysis plot for the resolved peaks of 3-Me-cp extracted from 1-R cage showing 14% *ee*.

(c) \pm 3-Me-cp with 1-S



Front Signal Results				
Retention Time	Area	Area %	Height	Height %
18.676	534751	58.09	121036	61.77
18.836	385745	41.91	74900	38.23
Totals	920496	100.00	195936	100.00

Figure S42. GC chromatogram and analysis plot for the resolved peaks of 3-Me-cp extracted from 1-S cage showing 16% *ee*.

4. Enantiomeric separation of 3-ethylcyclopentanone:

Column used: Supelco β -dex (30 m* 0.25 mm * 0.25 μ m),

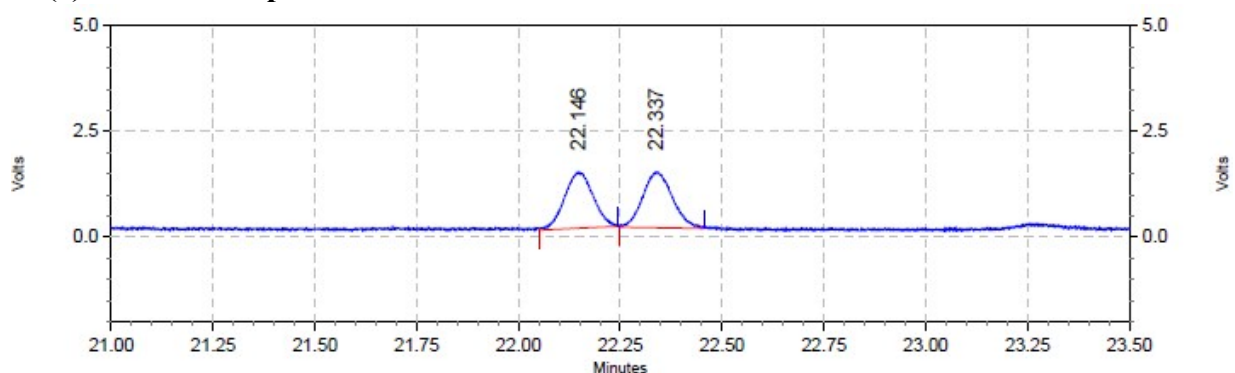
Split ratio 30:1,

Inlet temperature 210 $^{\circ}$ C,

Column pressure 7 psi

Temperature programme: started at 50 $^{\circ}$ C, and heated at the rate of 10 $^{\circ}$ C to 90 $^{\circ}$ C. It was further heated at the rate of 3 $^{\circ}$ C to 130 $^{\circ}$ C and hold for hold for 3 mins. Again it was heated at the rate of 2 $^{\circ}$ C to 150 $^{\circ}$ C. Finally it was heated at the rate of 10 $^{\circ}$ C to 210 $^{\circ}$ C.

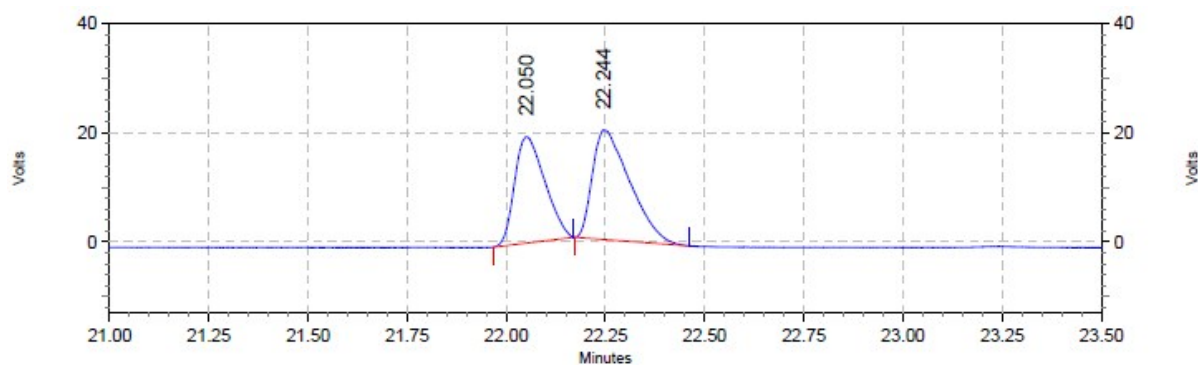
(a) Neat \pm 3-Et-cp:



Front Signal Results				
Retention Time	Area	Area %	Height	Height %
22.146	49496	49.17	10326	50.35
22.337	51160	50.83	10184	49.65
Totals				
	100656	100.00	20510	100.00

Figure S43. GC chromatogram and analysis plot showing the resolved peaks for rac-3-ethylcyclopentanone.

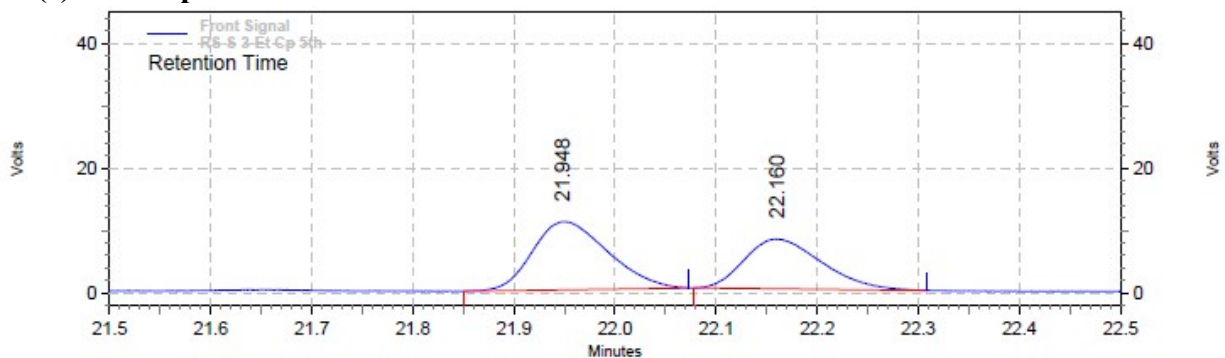
(b) \pm 3-Et-cp with 1-R:



Front Signal Results				
Retention Time	Area	Area %	Height	Height %
22.050	794248	43.93	149918	49.26
22.244	1013781	56.07	154401	50.74
Totals				
	1808029	100.00	304319	100.00

Figure S44. GC chromatogram and analysis plot for the resolved peaks of 3-Et-cp extracted from 1-R cage showing 12% ee.

(c) \pm 3-Et-cp with 1-S:



Front Signal Results				
Retention Time	Area	Area %	Height	Height %
21.948	434606	57.09	84147	57.77
22.160	326657	42.91	61504	42.23
Totals	761263	100.00	145651	100.00

Figure S45. GC chromatogram and analysis plot for the resolved peaks of 3-Et-cp extracted from **1-S** cage showing 14% *ee*.

Optical, spectral and structural data for guest-desorbed cages

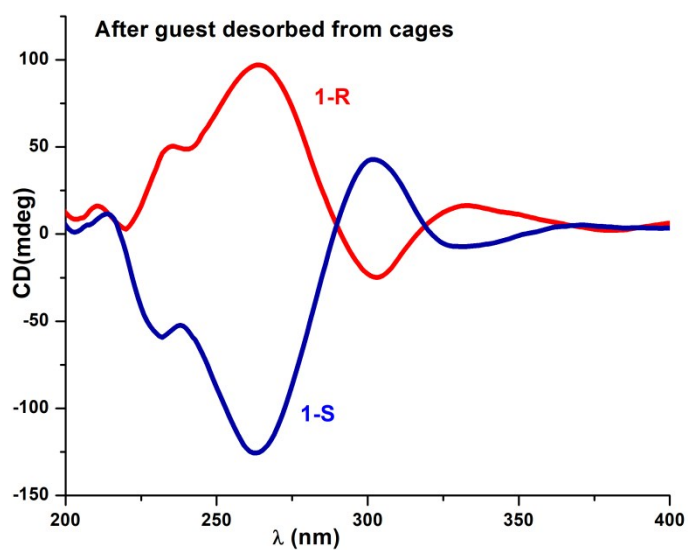


Figure S46. CD spectra of **1-R** and **1-S** cages obtained after desorbing bbl guest molecules.

Table S5: Specific rotation (α_D) values for cages **1-R** and **1-S** after desorbing bbl guests and its comparison with as-made samples

cages	α_D
1-R (as made)	+666°
1-R (after bbl desorp.)	+668°
1-S (as made)	-684°
1-S (after bbl dessorp.)	-679°

Table S6: Unit-cell parameters for the crystals obtained by re-crystallization after desorbing bbl guest molecules

1-R Crystal 1	1-R Crystal 2	1-R Crystal 3
a = 28.01 Å; $\alpha = 90^\circ$ b = 28.01 Å; $\beta = 90^\circ$ c = 28.01 Å; $\gamma = 90^\circ$ Volume = 21969 Å ³	a = 27.93 Å; $\alpha = 90^\circ$ b = 27.93 Å; $\beta = 90^\circ$ c = 27.93 Å; $\gamma = 90^\circ$ Volume = 21795 Å ³	a = 27.37 Å; $\alpha = 90^\circ$ b = 27.37 Å; $\beta = 90^\circ$ c = 27.37 Å; $\gamma = 90^\circ$ Volume = 20503 Å ³
1-S Crystal 1	1-S Crystal 2	1-S Crystal 3
a = 27.78(4) Å; $\alpha = 90^\circ$ b = 27.78 (4) Å; $\beta = 90^\circ$ c = 27.78 (4) Å; $\gamma = 90^\circ$ Volume = 21852 Å ³	a = 27.83(4) Å; $\alpha = 90^\circ$ b = 27.83(4) Å; $\beta = 90^\circ$ c = 27.83(4) Å; $\gamma = 90^\circ$ Volume = 21549 Å ³	a = 28.07(6) Å; $\alpha = 90^\circ$ b = 28.07 (6) Å; $\beta = 90^\circ$ c = 28.07(6) Å; $\gamma = 90^\circ$ Volume = 22124 Å ³

Supplementary References

- (1) B. Burns, N. P. King, H. Tye, J. R. Studley and M. Wills, *J. Chem. Soc., Perkin Trans. I*, 1998, **40**, 1027-1038.
- (2) G. M. Sheldrick, *Acta Crystallogr. C*, 2015, **71**, 3-8.
- (3) C. F. Macrae, P. R. Edgington, P. McCabe, E. Pidcock, G. P. Shields, R. Taylor, M. Towler and J. J. van de Streek, *J. Appl. Cryst.* 2006, **39**, 453-457.
- (4) (a) M. L. Connolly, *J. Mol. Graph.* 1993, **11**, 139-141; (b) L. J. Barbour, *Chem. Commun.* 2006, 1163-1168.
- (5) R. Kerssebaum, DOSY and Diffusion by NMR. In *User Guide for XWinNMR 3.5*, Version 1.0; Bruker Biospin GmbH: Rheinstetten, Germany, 2002.